Department of Food and Environmental Sciences
University of Helsinki
Finland

CEREAL β-GLUCAN IN AQUEOUS SOLUTIONS: OXIDATION AND STRUCTURE FORMATION

Noora Mäkelä

ACADEMIC DISSERTATION

To be presented, with the permission of the Faculty of Agriculture and Forestry of the University of Helsinki, for public examination in Walter hall, Viikki, on 10 November 2017, at 12 noon.

Helsinki 2017

Custos: Professor Vieno Piironen
Department of Food and Environmental Sciences
University of Helsinki, Finland

Supervisors: Docent Tuula Sontag-Strohm
Department of Food and Environmental Sciences
University of Helsinki, Finland

Docent Ndegwa Henry Maina
Department of Food and Environmental Sciences
University of Helsinki, Finland

Pre-examiners: Assistant Professor Athina Lazaridou
Department of Food Science and Technology
Aristotle University of Thessaloniki, Greece

Research Director Luc Saulnier
Biopolymers, Interactions & Assemblies Unit
French National Institute for Agricultural Research INRA, France

Opponent: Professor Sandra Hill
Division of Food Sciences
University of Nottingham, UK

ISBN 978-951-51-3683-1 (pbk.)
ISBN 978-951-51-3684-8 (PDF)
ISSN 0355-1180

Unigrafia
Helsinki 2017

“The important thing is not to stop questioning. Curiosity has its own reason for existing.”

-Albert Einstein

Abstract

Cereal (1→3)(1→4)-β-D-glucan, known as β-glucan, has both technological and physiological functionality related to its ability to increase viscosity in solutions. The viscosity is dependent on the molar mass, concentration and solubility of β-glucan, and thus any degradation during processing and storage may diminish its functionality. Quite recently, chemical oxidation was shown to be one factor leading to the degradation of β-glucan. The present study aimed to investigate the hydroxyl radical-mediated oxidation of cereal β-glucan, including the pathways and reaction products. Additionally, oxidised lipids were tested as a source of radicals in β-glucan oxidation. Finally, the physicochemical properties (e.g. aggregation and gelation) were studied in order to understand the influence of oxidation on functionality.

Hydrogen peroxide was shown to be the strongest oxidant, leading to both oxidative degradation and the formation of oxidised groups (e.g. carbonyl groups) within the chain. Additionally, oxidation of reducing end glucose units led to the formation of arabinose and formic acid. With ascorbic acid the oxidation was milder and mostly scission of β-glucan occurred. This difference was also seen in the aggregation behaviour, with very large but densely packed aggregates being formed when oxidising β-glucan with hydrogen peroxide. With ascorbic acid, fewer aggregates were formed and they could not be separated from single oxidised molecules during field-flow fractionation. This finding suggests the formation of cross-links via the oxidised groups in the molecules. The study showed for the first time that cereal β-glucan can be degraded by radicals from lipid oxidation although the oxidative degradation was significantly milder than with hydrogen peroxide.

The gelation of cereal β-glucan has been shown to be affected by the molar mass and structure (e.g. the ratio of DP3 and DP4 units) of β-glucan. However, former studies show gelation only at relatively high concentrations. In this study, gelation of barley and oat β-glucans (both native and oxidised) was shown with 1% and 1.5% solutions, respectively, when using optimised dissolution temperatures that resulted in partial solubilisation of β-glucan molecules. The partial dissolution was proposed to enable formation of nucleation cites for gelation.

In this study, changes in the structure and physicochemical properties of barley and oat β-glucans due to oxidation were demonstrated. Additionally, gelation of both non-oxidised and oxidised β-glucan was shown at concentrations relevant for food products. The results of this study provide an understanding of the role of oxidation for the stability of β-glucan in processing and storage of foods. The study suggests that gelation of β-glucan could overcome the negative effects of oxidation-related viscosity loss.

Acknowledgements

This study was carried out in the Cereal Technology Group at the Department of Food and Environmental Sciences, University of Helsinki. The work was funded by the Academy of Finland, the Finnish Food Research Foundation, and the August Johannes and Aino Tiura Research Foundation. Their financial support is greatly appreciated.

First, I want to express my deepest gratitude to my supervisors, Docent Tuula Sontag-Strohm and Docent Ndegwa H. Maina. I have been privileged to have the opportunity to work with you. It has been inspiring and I always felt that I had enough freedom to be able to grow as a researcher, while simultaneously, I never felt alone when dealing with the ups and downs of my thesis work.

During these past years, the winds of change have blown through our department (and also through the whole university). I am thankful to Professor Emeritus Hannu Salovaara, Professor Frederick Stoddard and Associate Professor Kati Katina for maintaining a good atmosphere in the Cereal Technology Group. You made it easy for us researchers to continue with our research work, despite the challenges with the ongoing changes.

I am sincerely grateful to Assistant Professor Athina Lazaridou and Dr. Luc Saulnier for the pre-examination of my doctoral thesis. Your comments and suggestions were valuable and constructive. I am thankful to my co-authors: Docent Anna-Maija Lampi, Docent Hannu Maaheimo, Professor Antje Potthast, Dr. Sonja Schiehser, Päivi Vikgren and Yujie Wang. I thank Professor Antje Potthast and Dr. Sonja Schiehser for hosting me in BOKU and teaching me about CCOA-labelling. Additionally, I want to thank my follow-up group, Dr. Reetta Kivelä and Dr. Marika Lyly. Adelaide Lönnberg is thanked for language revision of this thesis.

I have really enjoyed my journey during these years and it is for the large part due to the people around me. Thus, I want to express my gratitude to the colleagues who have been working in the Cereal Technology Group during this time: Outi Brinck, Dr. Xin Huang, Zhongqing Jiang, Dr. Päivi Kanerva and Yujie Wang. I thank Outi for all the assistance and help with many practical things. You never turned your back on any question or problem, but you were always eager to try to solve them. I am grateful to my colleague Marjo Pulkkinen who has shared with me this journey that began on our first day as food chemistry students in 2007. During these years I have really appreciated your peer support and all the discussions we have had.

I am thankful to my family, relatives and friends. I want to express my warmest thanks to my parents for always encouraging me and believing in me. Finally, I am grateful to Markus for his support and for being there for me during these years. I am privileged to have all of you in my life, and each of you have in your own way contributed to the succesful completion of this chapter of my life. For that, I am sincerely grateful.

Helsinki, September 2017

Noora Mäkelä

Contents

List of original publications

This thesis is based on the following publications:

I Mäkelä N, Sontag-Strohm T, Maina NH. 2015. The oxidative degradation of barley β-glucan in the presence of ascorbic acid or hydrogen peroxide. Carbohydr Polym 123:390–395.

II Mäkelä N, Sontag-Strohm T, Schiehser S, Potthast A, Maaheimo H, Maina NH. 2017. Reaction pathways during oxidation of cereal β-glucans. Carbohydr Polym 157:1769–1776.

III Mäkelä N, Maina NH, Vikgren P, Sontag-Strohm T. 2017. Gelation of cereal β-glucan at low concentrations. Food Hydrocolloids 73:60–66.

IV Wang Y-J, Mäkelä N, Maina NH, Lampi A-M, Sontag-Strohm T. 2016. Lipid oxidation induced oxidative degradation of cereal beta-glucan. Food Chem 197:1324–1330.

 They are referred to in the text by their Roman numerals.

Contribution of the author to papers I to IV:

I, II Noora Mäkelä planned the study together with the other authors and carried out most of the experiments. She had the main responsibility for interpreting the results and was the corresponding author of the papers.

III Noora Mäkelä planned the study together with the other authors. She had the main responsibility for the experimental work and interpreting the results. She was the corresponding author of the paper.

IV Noora Mäkelä planned the study together with the other authors. She shared the responsibility for the experimental work, interpreting the results and writing the article together with the other authors.

Abbreviations

β-glucan	(1→3)(1→4)-β-D-glucan
DP	Degree of polymerisation
DP3:DP4 ratio	The molar ratio of DP3 and DP4
AFM	Atomic force microscopy
CSLM	Confocal scanning laser microscopy
η	Viscosity
τ	Shear stress
$\dot{\gamma}$	Shear rate
η_{app}	Apparent viscosity
$[\eta]$	Intrinsic viscosity
$c_{[\eta]}^*$	Critical concentration
M_w	Weight average molar mass
G'	Storage modulus
G"	Loss modulus
SCFA	Short-chain fatty acids
LDL	Low-density lipoprotein
DSC	Differential scanning calorimetry
HPSEC	High performance size exclusion chromatography
AA	Ascorbic acid
ESR	Electron spin resonance
HPAEC-PAD	High performance anion exchange chromatography with pulsed amperometric detection
M_n	Number average molar mass
M_z	Z-average molar mass
M_w/M_n	Polydispersity index
GPC	Gel permeation chromatography
GFC	Gel filtration chromatography
V_h	Hydrodynamic volume
LS	Light scattering
RI	Refractive index
dn/dc	Refractive index increment
SLS	Static light scattering
DLS	Dynamic light scattering
MALS	Multi-angle light scattering
LALS	Low-angle light scattering
RALS	Right-angle light scattering
AsFlFFF	Asymmetrical flow field-flow fractionation
BBG	Barley β-glucan
OBG	Oat β-glucan

1 Introduction

Cereals are the most important food source all over the world (Kearney, 2010). Although the overall consumption of cereals calculated as a share of total consumed calories, which was 51% in 2001, is slowly declining (the average share is predicted to be 49% in 2030 and 47% in 2050), cereal products still have a significant dietary role (Alexandratos and Bruinsma, 2012; Kearney, 2010). At the same time, health awareness and functional food consumption are increasing, especially in industrialised countries (Kearney, 2010).

Dietary fibre has several positive effects on health. Review papers by Anderson et al. (2009), Buttriss and Stokes (2008) and Kaczmarczyk et al. (2012) list dietary fibre as having an effect on e.g. cardiovascular health, diabetes, inflammation, neurodegenerative diseases, obesity, gastrointestinal health and some cancers. However, oat and barley β-glucans are among the few dietary fibres that have approved health claims.

Cereal β-glucans are the major non-starch polysaccharides, especially in barley and oat, and are mainly located in endosperm and aleurone cell-walls in grains (Cui and Wood, 2000). β-Glucans consist of both water-extractable and water-unextractable glucans. The physiological functionality of cereal β-glucan has been sufficiently evidenced and thereby the interest towards this polysaccharide has increased. In 1997, the US Food and Drug Administration (FDA) was the first to approve health claim concerning oat soluble fibre reducing the risk of coronary heart disease, and in 2005 this was expanded to include barley as a suitable source of β-glucan (FDA, 1997, 2005). The European Food Safety Authority (EFSA) approved the first claim concerning cereal β-glucan in 2009, stating that it helps to maintain normal blood cholesterol, and in 2010 it approved a similar claim for oat β-glucan in reducing blood cholesterol (EFSA 2009, 2010b). The claim for a cholesterol-lowering effect was also accepted for barley β-glucan in 2011 (EFSA, 2011c). Additionally, in 2011 EFSA approved the claims that oat and barley β-glucans have a lowering effect on the postprandial glycaemic response, and that oat and barley fibres help increase faecal bulk (EFSA, 2011a, b).

The mechanisms for the physiological functionality of cereal β-glucans are thought to be based mainly on their ability to increase viscosity, which is related to both the molar mass and solubility of β-glucan (Wood, 2010). Consequently, degradation of β-glucan during processing and storage can be considered a threat to its physiological functionality. Degradation can occur through e.g. enzymatic or acid hydrolysis, alkaline degradation, pressure or heat treatments, or as recently shown by Kivelä et al. (2009a, b), also through chemical oxidation. In many food products the

components required for oxidation are present, since they contain metal ions for catalysis and typically the oxygen is also available. Reactive oxygen species can be formed from atmospheric oxygen, and radicals can also be formed in the presence of ascorbic acid (DeRosa and Crutchley, 2002; Kivelä et al., 2009a, b). Studies have shown loss of viscosity in β-glucan solutions due to oxidative degradation (Faure et al., 2012; Kivelä et al., 2009a, b; Paquet et al., 2010), and thus oxidation can lead to decreased functional properties of β-glucan.

In this thesis, the literature review gives an overall outline of cereal β-glucan, including its structure and physiological and functional properties, and describes the structure-function relationship. Degradation mechanisms are also reviewed, focusing more on oxidation, as well as the methodology used to study the oxidative degradation of β-glucan. The experimental part of the thesis focuses on oxidation extent and pathways paying special attention to the differences shown with different oxidants (H_2O_2, AA and oxidised lipids used in this study). The study aims to better understand changes in the β-glucan structure brought about by oxidation, and the consequent changes in its properties. It also attempts to link the structural information to the rheological properties, thus gaining further insight into the physiological and technological functionality of β-glucan.

2 Review of the literature

2.1 Cereal β-glucan

2.1.1 Structure of cereal β-glucan

β-Glucan is a major non-starch polysaccharide in oats and barley, and it is found in barley, oat, rye and wheat in concentrations of 3–11%, 3–7%, 1–2% and <1%, respectively (Cui and Wood, 2000). As shown in Fig. 1a, in oat groat (hulled grain) β-glucan is located mainly in the outer part of the groat, in the aleurone and sub-aleurone layers, and is therefore concentrated in the bran fractions during milling. In barley, however, it is spread throughout the groat, primarily in the cell walls of the endosperm (Fig. 1b). Several processing methods have been developed for concentrating β-glucan. They are classified as either wet or dry processes, and enable foodstuffs to be produced that contain up to 95% of β-glucan (Vasanthan and Temelli, 2008). Wet processes generally lead to higher purity than dry processes.

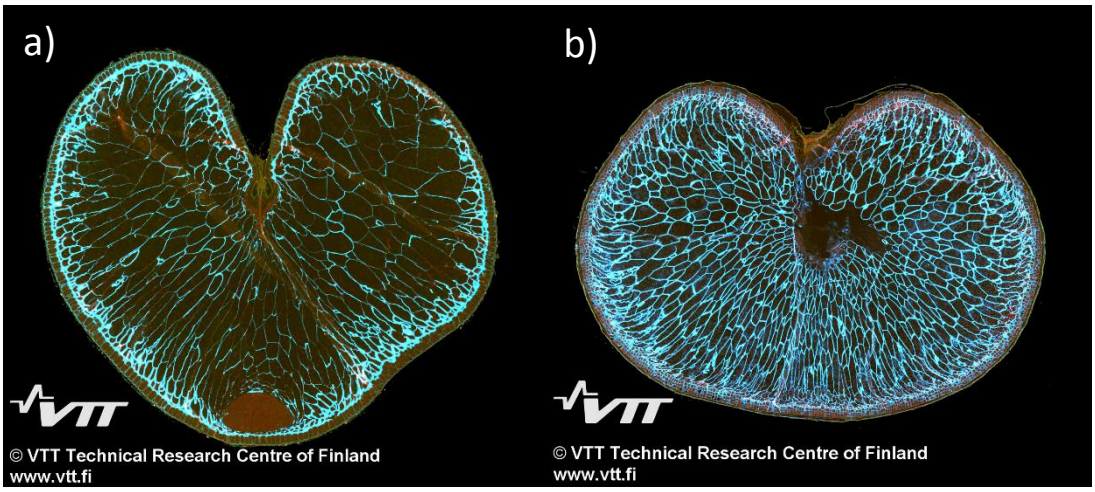

Figure 1. Microscopic cross-sections of oat (a) and barley (b) groats. β-Glucans in the cell walls are stained with Calcofluor and proteins with Acid Fuchsin. (Picture by Ulla Holopainen-Mantila, printed with permission of VTT Technical Research Centre of Finland)

The molar mass of β-glucan is altered significantly by extraction and analysis methods. This is seen in the high variation reported in different studies: 180 000–2 700 000 g/mol for oat β-glucan (Autio et al., 1992; Beer et al., 1997; Cui et al., 2000; Johansson et al., 2000; Skendi et al., 2003; Sundberg et al., 1996) and 450 000–2 500 000 g/mol for barley β-glucan (Beer et al., 1997; Cui et al., 2000; Gómez et al., 1997). Andersson and Börjesdotter (2011) studied the effects of genotype and environmental factors on the molar mass of oat β-glucan and found that the latter had

a significant effect, while genotype had only minimal impact. The content of β-glucan, however, was more influenced by the genotype.

In cereals, β-glucans occur as mixed-linkage (1→3)(1→4)-β-D-glucan (Scheme 1). It is composed of consecutive β-(1→4)-linked D-glucopyranosyl units that form cellulose-like segments, which are interrupted by single β-(1→3) linkages. These β-(1→3) linkages differentiate cereal β-glucan from cellulose and make the molecule more flexible and thus also water-soluble (Buliga et al., 1986). The β-(1→4)-linked segments are mainly composed of three (degree of polymerisation three, DP3) or four (DP4) glucose units, since they consist of about 91–93% and 92% of water-soluble oat and barley β-glucans, respectively (Doublier and Wood, 1995; Wood et al., 1994). However, also larger segments occur and about 7–9% of water-soluble β-glucans are DP5–9 and water-insoluble fractions may consist of cellulosic blocks of up to DP15. The molar ratio of DP3 and DP4 (DP3:DP4 ratio) in oat β-glucan varies from 1.7 to 2.4, in barley and rye β-glucans from 2.7 to 3.6, and in wheat β-glucan from 3.7 to 4.8, as reviewed by Wood (2010). The structural variation of β-glucans from different sources is linked to some differences in the functional properties, as explained later.

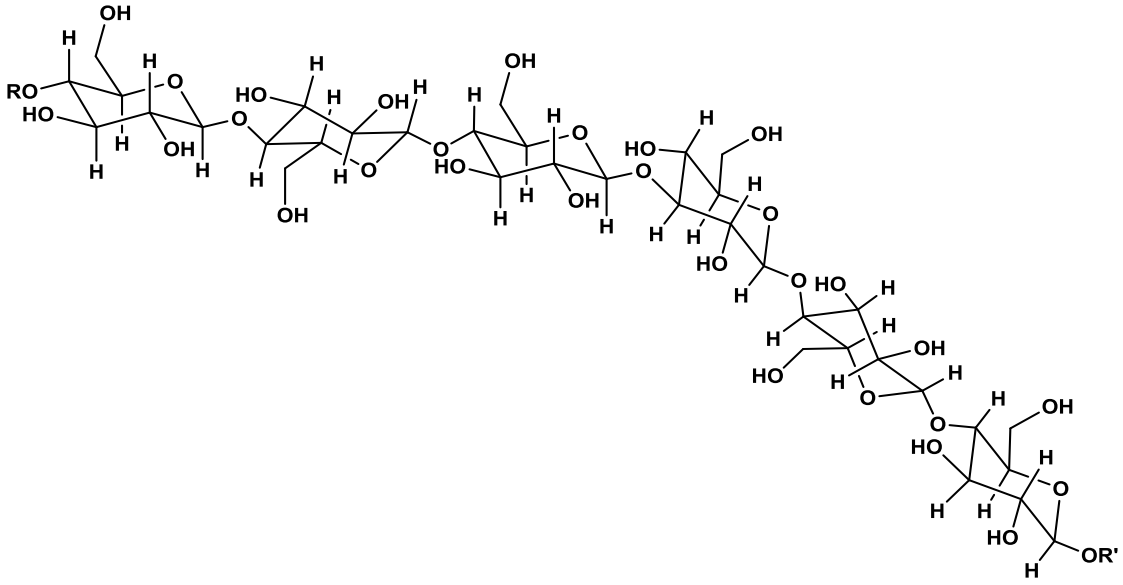

Scheme 1. β-Glucan structure. β-(1→3) linkages cause bending of the structure, which makes cereal β-glucans soluble in water.

2.1.1.1 Aggregation

A high DP3:DP4 ratio has been linked to lower solubility, possibly due to aggregation of β-glucan molecules via hydrogen bonding of regularly-repeated DP3 units that form junction zones between the molecules (Izydorczyk et al., 1998). Tvaroska et al. (1983) compared the crystallinity of barley β-glucan and lichenan, which also consists of β-(1→3) and β-(1→4)-linked glucose units but predominantly contains β-(1→4)-linked cellotriosyl (DP3) units, and thus has higher DP3:DP4 ratio than oat and barley β-glucans (Wood et al., 1994). Tvaroska et al. (1983) concluded that barley β-glucan, which has a less regular structure than lichenan, has a lower overall degree of crystallinity than lichenan.

Grimm et al. (1995) suggested a fringed micelle-type aggregation pattern for cereal β-glucans, where aggregates grow by side-to-side junctions of β-glucan molecules. The hydrodynamic volume of these aggregates increases only slightly with increasing molar mass, since the inner parts are packed to form stiff structures and only the outer parts have mobility. Wu et al. (2006) imaged the aggregation of oat β-glucan with atomic force microscopy (AFM) and confocal scanning laser microscopy (CSLM), showing an increase in aggregate size with increasing β-glucan concentration in water solutions. Additionally, Wu et al. (2006) performed AFM imaging of oat β-glucan dispersed with sodium dodecyl sulfate (SDS) and the results supported the aggregation pattern suggested by Grimm et al. (1995). According to Vårum et al. (1992), only some of the β-glucan molecules participate in aggregation. Even though the aggregating molecules represent a small numeral fraction, they may represent significant weight fraction, which can be visualised with light scattering techniques. However, as concluded by Vårum et al. (1992), aggregates are often not separated from single molecules by size exclusion chromatography, possibly because of the opening of the aggregates due to shear forces.

2.1.2 Rheological properties of aqueous β-glucan solutions

Rheology studies the flow and deformation of materials. Rheological measurements are divided roughly into the measurement of flow when a material is fluid and has viscous behaviour, and the measurement of deformation when a material is solid and has elastic behaviour. However, materials are seldom ideal fluids or solids, rather exhibiting both properties in which case they are considered viscoelastic.

2.1.2.1 Viscosity

Viscosity (η) describes the resistance of a fluid to flow, and can be studied by measuring its response to shear under a given stress. Under Couette flow, viscosity

(unit Pa·s) is presented as a ratio of shear stress (τ) to shear rate ($\dot{\gamma}$) as shown in Eq 1, where *F* is the applied force, *A* is the area, *v* is the velocity of the upper plate causing the shear, and *y* is the height of the sample.

$$\eta = \frac{F/A}{v/y} = \frac{\tau}{\dot{\gamma}} \quad \text{(Equation 1)}$$

If the viscosity of a material is constant with the changing shear rate, the material is called Newtonian. Polymer solutions may show Newtonian behaviour when the molar mass and/or concentration of the polymer is low (Picout and Ross-Murphy, 2003). For a Newtonian liquid, only one measurement point is enough to describe its viscosity, since the viscosity is independent of the shear rate. However, typically polymer solutions are considered non-Newtonian liquids, with viscosity varying with the shear rate (Picout and Ross-Murphy, 2003). For such materials, Eq. 1 is used for calculating the apparent viscosity η_{app} whereby the obtained viscosity value applies only to the used shear rate. When measuring the viscosity of a non-Newtonian material over a given shear rate range, the viscosity increases (shear-thickening, dilatancy) or decreases (shear-thinning, pseudoplasticity) with increasing shear rate. Random coil polysaccharide solutions are typically pseudoplastic, which is often caused by a decrease in viscosity due to the alignment of molecules in the direction of shear (Morris et al., 1981). However, when the polysaccharide concentration is high, pseudoplasticity can be caused by a decrease in cross-link density because of the disruption of entanglements due to the shear being faster than the formation of new entanglements.

During viscosity measurement, some viscosity loss can also occur due to structural changes of the sample material (Mewis and Wagner, 2009). These changes are indicated by a hysteresis loop when shear stress is plotted as a function of shear rate. Thixotropy is a phenomenon where viscosity decreases with time when flow is applied to a sample, and when the flow is discontinued the recovery shows some lag time. However, in thixotropic materials the changes are reversible, meaning that the viscosity always recovers with time. Some changes in materials due to flow can be irreversible and those materials will also show hysteresis even though they are not considered thixotropic.

Intrinsic viscosity (or limiting viscosity number, [η]) is a parameter that can be obtained for a polymer in dilute solutions where interactions between polymer molecules are minimal. The [η] value is related to *M* using the Mark-Houwink-Kuhn-Sakurada equation (Eq. 2), where *M* is molar mass and *K* and *a* are parameters that depend on the temperature and combination of polymer and solvent.

$$[\eta] = KM^a \quad \text{(Equation 2)}$$

The value *a* indicates the shape of the polymer in a specific solvent. The exponent *a* for oat and barley β-glucan is 0.71–0.81, as reviewed by Lazaridou et al. (2004). This indicates that β-glucan has an expanded coil conformation, since the exponent *a* has been reported to be 0.5–1.0 for expanded coils (Böhm and Kulicke, 1999a).

The critical concentration ($c_{[\eta]}$*) of a polymer solution can be calculated from the intrinsic viscosity (Böhm and Kulicke, 1999a). $c_{[\eta]}$* indicates the concentration at which the polymers are spread throughout the solvent volume but remain as single chains and not as an entangled network. Böhm and Kulicke (1999a) reported $c_{[\eta]}$* for barley β-glucan with a weight average molar mass (M_w) of 50 000 g/mol and 375 000 g/mol to be 2% and 0.5%, respectively. Doublier and Wood (1995) studied the rheological behaviour of non-hydrolysed and hydrolysed oat β-glucan solutions and demonstrated Newtonian behaviour at concentrations below 0.3%. When the concentration of non-hydrolysed oat β-glucan (1 200 000 g/mol) was increased, the solution became pseudoplastic and the shear-thinning behaviour became more distinct. The acid hydrolysed β-glucans (100 000 g/mol and 360 000 g/mol) were less viscous than the native form due to depolymerisation, but additionally their shear-thinning behaviour was somewhat different: In non-hydrolysed β-glucan, the decrease in η_{app} occurred only beyond a certain shear rate value, but in hydrolysed samples the viscosity decreased throughout the measured shear rate range. The increase in η_{app} with decreasing shear rate was suggested to be caused by a yield stress, which may arise from weak interactions between β-glucan molecules.

2.1.2.2 Gelation

Gels are viscoelastic materials, meaning that they have both viscous and elastic properties. The viscoelasticity of a material can be ascertained by sinusoidal measurement whereby an oscillating stress or strain is applied to the sample and the response is measured (Mitchell, 1980). The resulting mechanical spectrum shows both the storage modulus (*G'*) and loss modulus (*G''*) describing the elastic and viscous properties of the material, respectively. If a constant stress during oscillatory measurement is applied to an ideal elastic solid, the measured strain response would be in-phase with the applied stress (Fig. 2a). In the case of an ideal viscous liquid, the measured strain would be 90˚ out of phase (Fig. 2b). Viscoelastic materials have a phase difference between 0˚ and 90˚ (Fig. 2c).

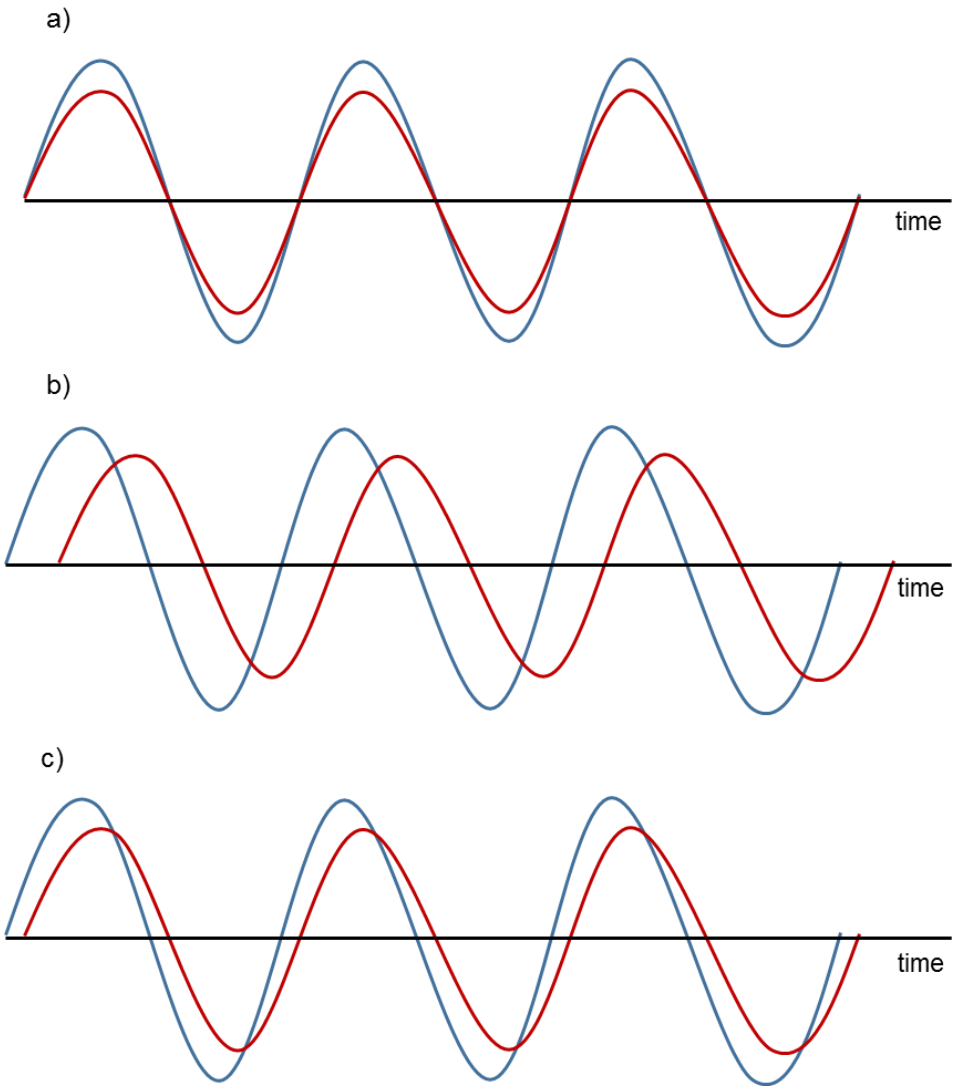

Figure 2. Stress (blue line) and strain (red line) are a) in-phase in the case of an ideal elastic solid, b) 90° out of phase in the case of an ideal viscous liquid and c) 0<x<90° in the case of a viscoelastic material.

Similarly to viscosity, gelation of β-glucan has also been shown to be concentration dependent (Böhm and Kulicke, 1999b). The induction period of gel formation is longer with decreasing concentration and simultaneously the gelation rate also declines. This is due to the higher probability of the molecules encountering, thus forming a gel network with increasing β-glucan concentration. In addition to the rate of gelation, the concentration affects the type of the gel, since the gel rigidity is influenced by the cross-link density. With increasing concentration the amount of cross-links per β-glucan chain is increased, and therefore the gel has higher rigidity.

Additionally, gelation susceptibility is influenced by the structural features of the β-glucans. A molar mass decrease is considered to increase the gelation rate, which

has been explained by the higher mobility of the smaller molecules (Böhm and Kulicke, 1999b; Doublier and Wood, 1995). Another structural factor related to gelation is the length of cellulosic segments in β-glucan molecules. Formation of some junction zones between β-glucan molecules is needed to form aggregates or a gel network. Aggregation of β-glucan has been suggested to be caused by the formation of micelle-like structures, as described in 2.1.1.1, but as Li et al. (2011) clarified, these kinds of structures cannot grow to form a gel network. Thus, in gelation the formation of junction zones must be somewhat different. According to Fincher and Stone (1986), the formation of polysaccharide gels requires junction zones, and the rigidity of the gel is affected by the amount and length of these zones. In β-glucan, particularly, the junctions formed via hydrogen bonding were suggested to be formed by the longer cellulosic blocks with several consecutive β-(1→4) linkages in the structure (Fig. 3a). However, a more recent theory on the mechanism of β-glucan gelation is based on the repeated cellotriosyl units in the molecules, shown in Fig. 3b (Böhm and Kulicke, 1999b). This theory is supported by the finding that gelation susceptibility increase in the order oat β-glucan < barley β-glucan < wheat β-glucan < lichenan, since the DP3:DP4 ratios are 1.7–2.4, 2.7–3.6, 3.0–4.5 and >20, respectively (Böhm and Kulicke, 1999b; Cui et al., 2000; Cui and Wood, 2000; Lazaridou et al., 2004; Tosh et al., 2004a; Wood, 2010).

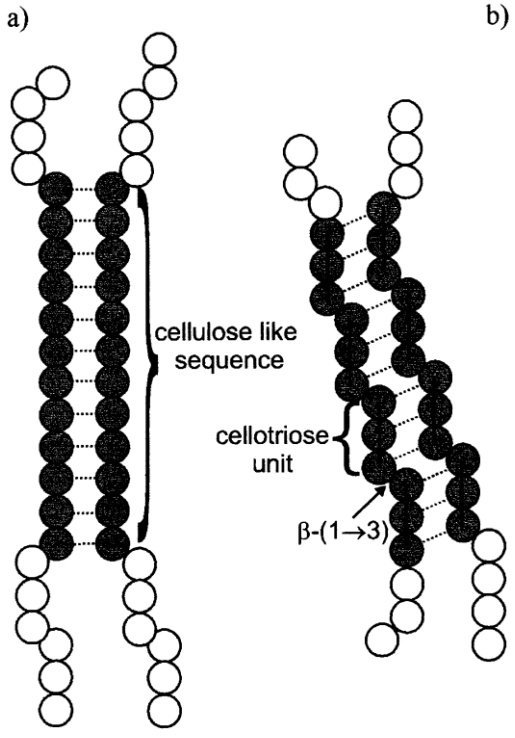

Figure 3. a) A model suggesting aggregation of β-glucan through cellulosic blocks formed by several consecutive β-(1→4) linkages in the structure, and b) a model proposing aggregation via repeated cellotriosyl units in the β-glucan structure. Adapted from Böhm and Kulicke (1999b), copyrights (1999) Elsevier Science Ltd.

2.1.3 Physiological functionality of cereal β-glucan

Dietary fibres can be categorised by different factors. Often they are classified as water-soluble or water-insoluble, but this does not directly describe their functionality. Classification based on viscosity and fermentability is more convenient when discussing physiological functionality (Kaczmarczyk et al., 2012). The solubility of cereal β-glucans varies depending on the source. Oat and barley β-glucans are classified as soluble dietary fibres, although a minor part of them are insoluble, or more correctly unextractable, in water (Wood, 2010). In rye and wheat, most of the β-glucans are water-unextractable (Cui et al., 2000; Ragaee et al., 2008).

The European Food Safety Authority, EFSA, defines dietary fibres as consisting of non-digestible carbohydrates and additionally lignin (EFSA, 2010a). Thus, non-starch polysaccharides (including cellulose, hemicelluloses, pectins and hydrocolloids) are considered dietary fibres, as are resistant starch, fructo-oligosaccharides, galacto-oligosaccharides and other resistant oligosaccharides. Dietary fibres act in digestion as bulking agents, increase the gut transit rate, and can be at least partly fermented by colon microbes to form short-chain fatty acids (SCFA), acetate, butyrate and propionate (Buttriss and Stokes, 2008; Scott et al., 2008). The ratio of these compounds depends on the kinds of substrates (i.e. fermentable dietary fibre) that reach the colon, since the gut microbiota is altered by the dietary fibre composition, and the type of SCFAs produced by different gut microbes varies (Kaczmarczyk et al., 2012; Scott et al., 2008). SCFAs are beneficial for colon health due e.g. to their pH-lowering capacity, which inhibits the growth of pathogenic microbes (Buttriss and Stokes, 2008). Studies have also shown that high consumption of dietary fibres can reduce the risk of obesity (Anderson et al., 2009). Dietary fibres increase satiety, and although the mechanism is still somewhat unclear, it may be linked to their effect on gut hormone secretion. Additionally, studies on dietary fibres and the risk of colorectal cancer are contradictory and the results controversial, as discussed by Bingham et al. (2003). In a study by Bingham et al. (2003), total dietary fibre consumption was shown to correlate negatively with the risk of colorectal cancer, but it was emphasised that the high fibre foods used in the study consist of many other nutrients and phytochemicals that may have a role in the prevention of colorectal cancer.

There is some evidence for dietary fibres promoting cardiovascular health and preventing diabetes. However, there are no joint health claims for all the dietary fibres concerning these physiological functionalities. Cereal β-glucans are one of the few dietary fibres with health claims approved by EFSA and FDA (EFSA 2010b, 2011a, b, c; FDA 1997, 2005). As reviewed by Mälkki and Virtanen (2001), the ability of β-glucan to increase luminal viscosity may affect through several mechanisms. These include hindering nutrient absorption and decreasing enzymatic hydrolysis due to retarded contact between the enzymes and the substrates. Wood et al. (1994)

showed that the effect of β-glucan on post-prandial plasma glucose levels decreased with decreasing viscosity. The mechanism for the ability of β-glucan to lower the postprandial glucose response is linked to the molar mass and solubility of β-glucan, which determine its viscosity in solution (Wood, 2010). The definite mechanism behind the cholesterol-lowering effects remains somewhat unclear, however, as stated by EFSA, it could also be related to the viscosity of β-glucan in the small intestine, which might inhibit the absorption of bile acids (EFSA, 2010b, 2011c). This would lead to the synthesis of bile acids from cholesterol in the liver reducing blood cholesterol levels. Additionally, an increase in viscosity of the intestinal digest, may hinder cholesterol absorption directly (Othman et al., 2011). Othman et al. (2011) considered that the form of the food containing β-glucan may be a vital factor for the cholesterol-lowering effect. In reviewed studies, a clear reduction in low-density lipoprotein (LDL) cholesterol was observed after consumption of liquid foods containing β-glucan, but the results for solid matrices were controversial. One proposed reason for the conflicting results is the possible degradation of β-glucan during processing.

2.2 Degradation of cereal β-glucan

In food processing, several factors can lead to the degradation of cereal β-glucans. For instance, bread baking involves enzymes (from flour and from yeast if the dough is fermented), heat treatment and possibly some oxidants, all of which can cause some loss of molar mass of β-glucans. Since the viscosity of β-glucans affects both the technological properties and physiological functionality, it is necessary to consider the different causes of degradation when developing food products containing β-glucan.

2.2.1 Enzymatic degradation

Grains contain endo- and exohydrolases, which can degrade cell-wall β-glucans in cereal grains during growth and development of the plant (Hrmova and Fincher, 2001). The main groups of β-glucan endohydrolases present in germinating cereal grains are (1→3)(1→4)-β-glucan 4-glucanohydrolase (lichenase, EC 3.2.1.73), (1→4)-β-glucan 4-glucanohydrolase (cellulase, EC 3.2.1.4) and (1→3)-β-glucan 3-glucanohydrolase (EC 3.2.1.39). Additionally, exo-β-glucanase activity has been observed in barley grains, as reviewed by Fincher (1989). Two different (1→3)(1→4)-β-glucanase isoenzymes have been isolated from barley, one of which is also found in vegetative plant tissue while the other is specific to germinated grains (Fincher, 1993).

Enzymatic degradation of cereal β-glucans can occur during baking. Åman et al. (2004) observed degradation of oat bran β-glucan during wheat bread baking. Since in their study the oat bran had been heat treated and endogenous enzymes thus inactivated, they suggested that the enzymatic degradation was due to either enzymes in yeast or in wheat flour (e.g. β-glucanases). However, yeast addition was not shown to have an effect on the molar mass of barley β-glucan in baking trials by Andersson et al. (2004). They were using mixtures of barley and wheat flours and concluded that the degradation was mainly caused by the endogenous β-glucanases in flours. Lazaridou et al. (2014) showed a decrease in viscosity of barley flour slurries due to β-glucanase activity. In slurries prepared from non-autoclaved barley flour the loss of viscosity was rapid, but it was hindered or totally inhibited in slurries made of autoclaved barley flours depending on the moisture content of the flour during autoclaving.

2.2.2 Thermal degradation

Thermal degradation of polysaccharides has been extensively investigated, but studies on β-glucan degradation due to heat treatments are scarce. The chemical bonds in polymers can be cleaved if the dissociation energy is overcome when heating the polymers (Pielichowski and Njuguna, 2005). The thermal stability of different polysaccharides can be linked to their structural and functional group differences (Zohuriaan and Shokrolahi, 2004). According to Pielichowski and Njuguna (2005), thermal degradation of polymers includes three different mechanisms: scission of the side-groups, depolymerisation and random scission.

Villetti et al. (2002) suggested the effect of heating on the structure of polysaccharides to be stepwise. Lower temperatures cause scission of exocyclic groups and change in conformation, while actual cleavage of the polysaccharide chain requires higher temperatures. Thermogravimetric measurement was conducted at a heating rate varying from 5 to 20°C/min and the maximum degradation temperatures for methyl cellulose, xanthan and sodium hyaluronate were reported to be 376°C, 298°C, and 276°C, respectively. Zohuriaan and Shokrolahi (2004) also studied the effect of thermal treatment (heating rate 20°C/min) on various polysaccharides (arabic gum, tragacanth gum, xanthan gum, sodium alginate, chitosan, sodium carboxymethyl cellulose, hydroxyethyl cellulose and methyl cellulose) and showed an intense exothermic peak in differential scanning calorimetry (DSC) measurements at around 300°C. Based on thermogravimetric analysis, they reported the main decomposition of the studied polysaccharides to start at temperatures above 200°C, and methyl cellulose at a significantly higher temperature (decomposition starting at 325°C), which supported the results of Villetti et al. (2002). Bradley et al. (1989) showed a reduction in M_w of guar gum from 700 000 g/mol to 160 000 g/mol when heating the

solution only at 110°C for 12 min. However, Wang et al. (2001) indicated that the decrease in viscosity and M_w during autoclaving (120°C, 15 min) of detarium xyloglucan was due to a reduction in aggregation rather than depolymerisation. They emphasised, however, that based solely on the M_w measurement by high performance size exclusion chromatography (HPSEC), it was not possible to differentiate whether the M_w decrease was due to cleavage of the chain or disruption of the aggregates.

A study on the thermal degradation of both neutral and charged polysaccharides has shown that neutral polysaccharides are more resistant to thermal degradation than ionic polysaccharides (Villetti et al., 2002). Thus, neutral β-glucan could be considered to be moderately stable in processes where heating is involved. Interestingly, studies on the degradation of detarium xyloglucan, dextran and oat β-glucan during autoclaving have shown differences in the behaviour of these polysaccharides. Wang et al. (2001) showed only disaggregation when detarium xyloglucan and dextran were heated at 120°C for 15 min, but with oat β-glucan both disaggregation and depolymerisation occurred. The reason for this difference is somewhat unclear, but the possibility of some oxidative degradation occurring during heating of the oat β-glucan extract cannot be fully excluded.

2.2.3 Acid hydrolysis

Acid hydrolysis is a reaction catalysed by a compound that is able to donate protons (H^+). The reaction includes cleavage of the glycosidic bond in polysaccharides with the addition of a water molecule (H^+ and hydroxyl ion, OH^-) resulting in two stable products. In β-glucan, acid hydrolysis can cause cleavage of either β-(1→3) or β-(1→4) linkages. The randomness of this cleavage is uncertain, but the results of Tosh et al. (2004b) indicate that the scission of these two linkage-types would not occur completely randomly.

Acid hydrolysis of β-glucan has been shown to be affected by pH, temperature and reaction time (Vaikousi and Biliaderis, 2005). Molar mass seems to affect the hydrolysis reaction, since Vaikousi and Biliaderis (2005) observed that for higher molar mass β-glucan (molar mass = 250 000 g/mol) the effect on viscosity was more pronounced and the reaction time was the major factor affecting the extent of the hydrolysis, while for lower molar mass β-glucan (molar mass = 140 000 g/mol) the pH was the most influential factor.

Compared to enzyme-hydrolysed β-glucans, more free glucose is produced during acid hydrolysis (Tosh et al., 2004b). In a study by Johansson et al. (2006), acid hydrolysis yielded mainly glucose already after a 1-h reaction time at a high reaction temperature (120°C). The hydrolysis was shown to be highly dependent on the

reaction temperature, since at 70°C the amount of glucose was significantly lower and at 37°C no hydrolysis products were detected during a 12-hour reaction time. Similar temperature effects have been shown with guar gum by Wang et al. (2000). They showed minor degradation (2.2% viscosity loss) when guar gum was incubated at pH 1.5 at 25°C for 4 h while at 50°C the depolymerisation was faster (36.7% viscosity loss). They also concluded that the effect of temperature was more significant with lower pH values. At pH 3.0, no significant viscosity loss (2.8%) was observed even at 50°C, and thus the results indicate that complete acid hydrolysis requires both relatively low pH and elevated temperature.

2.2.4 Alkaline degradation

Reactions of polysaccharides in alkaline conditions include peeling, stopping reactions and alkaline hydrolysis, and the occurrence of these reactions is dependent on the reaction temperature. At temperatures below 170°C, alkaline conditions may cause degradation of polysaccharides through peeling reactions at reducing ends, known also as endwise degradation (Knill and Kennedy, 2003). Peeling reactions are mostly studied in the case of cellulose, where elimination reactions can lead to the cleavage of β-(1→4) linkages. In cellulose, β-elimination at the C4 position leads to cleavage of the reducing-end glucose and consequent formation of saccharinic acids (Knill and Kennedy, 2003; Pavasars et al., 2003). However, if β-elimination in cellulose occurs at some other carbon than C4, the glucose unit will remain attached to the cellulose molecule, and the peeling reaction will be terminated (known as stopping reactions). Luchsinger and Stone (1976) studied the peeling reactions of oligosaccharides composed of D-glucose units linked by β-(1→4) and β-(1→3) linkages and showed faster peeling of β-(1→3)-linked glucose residues than β-(1→4)-linked glucose residues. This probably would lead to some differences in the peeling of cereal β-glucan with both β-(1→3) and β-(1→4) linkages compared to cellulose with only β-(1→4) linkages.

At temperatures above 170°C, random alkaline hydrolysis of cellulose causing scission of the chain and significant molar mass decrease has been observed (Knill and Kennedy, 2003). Alkaline scission leads to the formation of new reducing ends, and thus the consequent peeling reactions further increase the rate of molar mass decrease.

Alkaline degradation of β-glucan is not likely to occur in food products, but rather during extraction processes where different alkalis are used for efficient extraction. Bhatty (1995) studied the effect of alkaline concentration on the solubility of β-glucans and showed increasing extractability of β-glucans from hull-less barley and oat brans with increasing NaOH concentration until the maximum was reached at 0.75 M NaOH.

In that study, NaOH was concluded to be an efficient solvent for β-glucan extraction. However, alkaline extraction of β-glucan may lead to decreased viscosity, indicating degradation of the molecule in alkaline conditions (Ahmad et al., 2010).

2.2.5 Chemical oxidation

Oxidation reactions in foods can be roughly divided into lipid-phase and aqueous-phase oxidation. Lipid-phase oxidation reactions are usually initiated either by exposure to light and the consequent photosensitisation, by the action of oxidising enzymes or through metal-catalysed reactions (Skibsted, 2010). In the aqueous phase there are some lipid radicals causing oxidative stress, but additionally, oxidation can be initiated by the action of reactive oxygen species (ROS).

In most food products, all the components needed for initiation of oxidation are already present. Oxidation reactions in foods typically occur via metal-catalysed reaction pathways (Kanner, 2010). Iron is a common metal catalyst present in foods and it occurs mainly in ferrous (Fe^{2+}), ferric (Fe^{3+}) or ferryl (Fe^{4+}) forms. Additionally, oxygen is present in most food processes. Atmospheric oxygen (O_2) itself is not very reactive, but there are several ROS compounds that can be formed from it. These oxygen species can cause oxidative degradation of different macromolecules (including polysaccharides) in foods.

2.2.5.1 Radical formation

Reactive oxygen species (ROS) include e.g. singlet oxygen and oxygen radicals (including superoxide and hydroxyl radicals). Singlet oxygen can be formed from ground-state (triplet-state) oxygen (O_2) by different mechanisms. In a photosensitisation reaction, singlet oxygen is formed from O_2 with light and a photosensitiser that absorbs the energy of the light and excites the oxygen to the singlet state (DeRosa and Crutchley, 2002). A superoxide radical with one unpaired electron (O_2^-) is formed from O_2 by the addition of a single electron and this reaction can be catalysed by transition metals (Reaction 1) (Halliwell and Gutteridge, 1984; Kanner, 2010). If another electron is added to the formed O_2^-, a peroxide ion (O_2^{2-}) is produced (Halliwell and Gutteridge, 1984). O_2^{2-} readily produces hydrogen peroxide (H_2O_2) depending on the pH, and since the pK_a value of H_2O_2 is 11.7, in most of the reaction conditions it occurs in its protonated form. Additionally, H_2O_2 can be formed from O_2^- in a dismutation reaction (Reaction 2) (Halliwell and Gutteridge, 1984).

$$Fe^{2+} + O_2 \rightarrow Fe^{3+} + O_2^- \quad \text{(Reaction 1)}$$

$$2O_2^- + 2H^+ \rightarrow H_2O_2 + O_2 \quad \text{(Reaction 2)}$$

Hydrogen peroxide may decompose to form hydroxyl radicals (OH•) as described in 1894 by Fenton who observed the catalytic role of iron when oxidising tartaric acid with H_2O_2 (Fenton, 1894). The combination of H_2O_2 and ferrous iron as a catalyst, is called Fenton's reagent. Haber and Weiss (1934) studied the decomposition of H_2O_2 in the presence of iron, and showed that the decomposition is a chain reaction (Reactions 3-6) in which two radicals are formed: OH• and a hydroperoxyl radical, $HO_2^{\bullet}$.

$Fe^{2+} + H_2O_2 \rightarrow Fe^{3+} + OH^- + OH\bullet$ (Reaction 3)
$OH\bullet + H_2O_2 \rightarrow H_2O + HO_2^{\bullet}$ (Reaction 4)
$HO_2^{\bullet} + H_2O_2 \rightarrow O_2 + H_2O + OH\bullet$ (Reaction 5)
$OH\bullet + Fe^{2+} \rightarrow Fe^{3+} + OH^-$ (Reaction 6)

Reaction 3 (Fenton reaction) is an initiation step and Reaction 6 terminates the chain. Barb et al. (1951) presented another additional termination reaction (Reaction 7):

$Fe^{2+} + HO_2^{\bullet} \rightarrow Fe^{3+} + HO_2^-$ (Reaction 7)

Later, some alternatives for radical-mediated oxidation reactions were found, since the formation of FeO^{2+} has been suggested to form as an intermediate in oxidation reactions (Barbusinski, 2009; Kremer, 2003; Qian and Buettner, 1999). According to Qian and Buettner (1999), the initiation pathway depends on the concentration of oxygen and hydrogen peroxide. They indicated that the Fenton reaction (Reaction 3) is the major initiator of the oxidation when the concentration of O_2 is less than 10-fold that of H_2O_2 (Qian and Buettner, 1999). However, if the concentration of O_2 is much higher (at least 100-fold), Reaction 1 is favoured. In these kinds of conditions Qian and Buettner (1999) suggested the Fenton reaction to play a minor role in oxidation, and initiation would occur mostly through the formation of Fe^{2+}-dioxygen complexes. Løgager et al. (1992) studied the formation of FeO^{2+} from Fe^{2+} and ozone (O_3), and further reactions of FeO^{2+}. They suggested that FeO^{2+} can interact with H_2O_2 to form $HO_2^{\bullet}$ (Reaction 8), and further reaction of $HO_2^{\bullet}$ with FeO^{2+} will produce O_2 (Reaction 9).

$FeO^{2+} + H_2O_2 \rightarrow Fe^{3+} + HO_2^{\bullet} + OH^-$ (Reaction 8)
$FeO^{2+} + HO_2^{\bullet} \rightarrow Fe^{3+} + O_2 + OH^-$ (Reaction 9)

Walling (1998) discussed the possibility of different intermediates in Fenton-type reactions involving hydrogen peroxide and a metal catalyst. It was concluded that even though the mechanism including the formation of ferryl species has recently been presented, there is evidence suggesting that oxidation often seems to follow the mechanism with formation of intermediate hydroxyl or alkoxyl radical oxidants. In a review by Barbusinski (2009), the effect of pH on the intermediates was emphasised,

as it was presumed that at low pH the oxidation would proceed via the radical pathway including the formation of OH•, but at high pH the non-radical pathway would dominate with formation of ferryl ions.

Hydroxyl radicals can also be formed by the action of ascorbic acid (AA). Ascorbate (AA^-) is a commonly known antioxidant, which can scavenge radicals ($X^•$) by one-electron transfer forming a relatively stable ascorbate radical ($AA^{•-}$) (Reaction 10, Duarte and Lunec, 2005).

$$AA^- + X^• \rightarrow AA^{•-} + XH \qquad \text{(Reaction 10)}$$

The effect of ascorbic acid (either as AA or AA^- depending on pH) is concentration dependent and the antioxidant effect is seen only when the concentration of AA is high enough. The damaging effect of AA on DNA has been studied and the damage was shown to be more severe with increasing AA concentration (Guo et al., 2002). Interestingly, beyond a certain level the increase in AA concentration led to a reduced damaging effect. This was suggested to be caused by the existence of a concentration threshold, above which AA becomes an antioxidant. At concentrations below the threshold, AA can cause oxidation of polymers. AA can be oxidised in the presence of a metal catalyst to form an ascorbyl radical with the simultaneous formation of H_2O_2 from molecular oxygen and reduction of the metal catalyst. This H_2O_2 can be used in the Fenton reaction (Reaction 3) to form hydroxyl radicals. Fry (1998) showed prevention of AA induced oxidation with the addition of catalase enzyme, which degrades H_2O_2 to H_2O and O_2. This indicates that oxidation with AA entails initial formation of H_2O_2 and consequent Fenton reaction.

2.2.5.2 Oxidation of β-glucan

Highly reactive OH• attacks the substrate molecule randomly, leading to abstraction of carbon-bound hydrogen or addition to double bonds of the structure (Arts et al., 1997). In a reaction between glucose and OH•, there are six possible radicals, since hydrogen abstraction can occur at any of the six C-H moieties (Schuchmann and von Sonntag, 1977). The abstraction of hydrogen often leads to rearrangement reactions, one example being the elimination of water from carbohydrates in acidic and alkaline conditions (Arts et al., 1997; von Sonntag, 1980). For example, if hydrogen is abstracted from the C2 position of glucose in acidic conditions, the formed radical is shifted from C2 to an axial carbon C1, with consequent formation of a carbonyl group at the C2 position and loss of H_2O (Arts et al., 1997). The reaction of carbohydrate radicals with O_2 can lead to formation of peroxyl radicals. Consequently, the rate of the rearrangement reactions and peroxyl radical formation determines the pathway that oxidation follows if oxygen is available (von Sonntag, 1980). Some possible reaction pathways of radical-mediated oxidation are presented in Scheme 2.

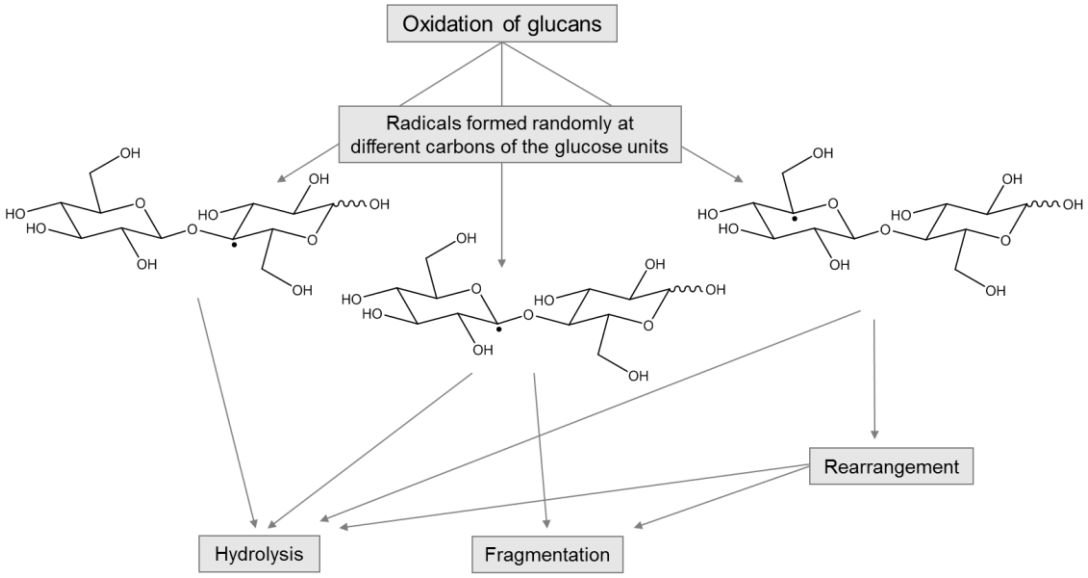

Scheme 2. Examples of oxidation pathways of glucan structures (modified from Kivelä, 2011; von Sonntag, 1980).

In polysaccharides, oxidation often leads to cleavage of the chain. In a review by von Sonntag (1980), the oxidation of cellobiose was indicated to form radicals mainly at positions C1, C4 and C5, all of these leading to scission of the glycosidic linkage. The reactions during cleavage of the glycosidic linkage include hydrolysis, fragmentation and/or rearrangement. Gilbert et al. (1984) studied the oxidation reactions of dextrans using electron spin resonance (ESR) spectroscopy and indicated rearrangement of the original radical species due to the lowered pH. These rearrangements cause glycosidic cleavage, e.g. scission of the α-(1→6) linkage by rearrangement of the radical at C2 to C1, with consequent formation of a carbonyl group at C2. Rearrangement of C4 radicals to the C3 position was suggested to cause also scission of the side chains linked by α-(1→3) linkages.

Previously, degradation of cereal β-glucan during processing has been attributed mainly to enzymatic or acid hydrolysis, but quite recently Kivelä et al. (2009a) reported degradation of oat and barley β-glucan due to oxidation. They showed that both the viscosity and M_w of β-glucans decreased significantly already 2 h after treatment with 10 mM AA and added ferrous ions (Fe^{2+}). Faure et al. (2012) studied the formation of hydroxyl radicals with ESR and confirmed that the viscosity loss of β-glucan with added AA and Fe^{2+} was due to radical-mediated oxidation. Some radicals were formed even in the absence of AA with added Fe^{2+}, and this was suggested to be initiated by superoxide formation during the reaction of Fe^{2+} and O_2 (Reaction 1).

In a study by Kivelä et al. (2009b), oxidation of β-glucan was shown to be dependent on the oxidant concentration, since the viscosity loss of oat β-glucan extract at pH 4.8 was 30%, 75% and 90% with 2 mM, 4 mM and 10 mM AA, respectively. However,

with 50 mM AA the molar mass decrease of β-glucan has been shown to be less than with 10 mM AA, and the suggested reason is the antioxidativity of AA at higher concentrations (Kivelä et al., 2012). Also the effect of Fe^{2+} concentration in oxidation of barley β-glucan with AA has been studied by Faure et al. (2013), and an increase in Fe^{2+} content did not significantly affect the viscosity loss of β-glucan. All AA-containing samples with added Fe^{2+} showed higher viscosity loss than the sample without iron addition, but no difference was observed between samples having 50 µm, 200 µm, 500 µm or 1 mM Fe^{2+}.

2.3 Analysis of the macromolecular properties of β-glucan

2.3.1 Analysis of the structural components of β-glucan

Usually, polysaccharide structure analysis includes complete hydrolysis to gather information about the different monosaccharide building blocks and their relative amounts. β-Glucan is a homopolysaccharide, since it is composed of glucose units only. However, there are some structural differences in β-glucans from different cereal grains. These differences include the length of the cellulosic segments and especially the DP3:DP4 ratio (Lazaridou and Biliaderis, 2007). The distribution of different DPs in the structure of β-glucan is studied by hydrolysing the molecule with lichenase enzyme. Lichenase cleaves specifically the β-(1→4) linkage that follows the β-(1→3) linkage, resulting in the oligosaccharide structures described in Fig. 4. However, there is some suggestion of lichenase-stable structures, as proposed by Simmons et al. (2013) who showed the occurrence of a lichenase-stable hexasaccharide in barley β-glucan.

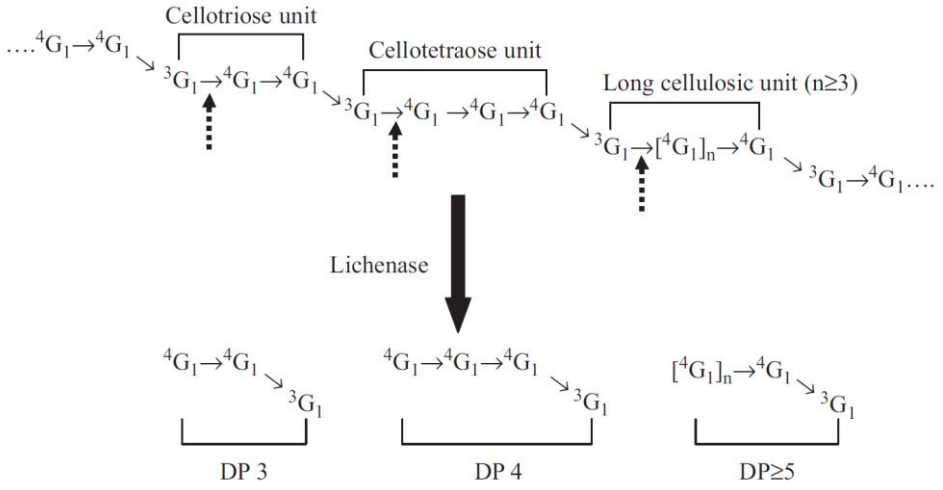

Figure 4. Oligosaccharides formed during enzymatic hydrolysis of cereal β-glucan with lichenase. Adapted from Lazaridou and Biliaderis (2007), copyrights (2007) Elsevier Ltd.

Oligosaccharides released by enzymatic hydrolysis can be analysed using high performance anion exchange chromatography with pulsed amperometric detection (HPAEC-PAD). In the HPAEC method, alkaline eluent is used to get weakly acidic carbohydrates (pK_a values 12–14) in oxyanion form (Corradini et al., 2012; Lee, 1990). Thus, even neutral carbohydrates can be separated and eluted using anion exchange chromatography. The separation is based on slight differences in the acidity of hydroxyl (OH) groups at different positions in the carbohydrate ring structure, e.g. the anomeric OH group at position C1 being the most acidic in the glucose structure. Detection with PAD usually involves a gold electrode and a repeating three-step potential sequence (Corradini et al., 2012). The detection occurs during the first step, where the detection potential is kept constant for a certain time period, during which the current from carbohydrate oxidation is measured. At the second step, the electrode is cleaned from impurities by oxidising with a positive potential. During the third step a negative potential is applied to reduce the electrode.

2.3.2 Molar mass distribution

The molar mass of β-glucan is often a subject of interest, since it is linked to the physiological and technological properties. Instead of one specific molar mass, β-glucans (as with other polysaccharides) have a distribution of molar masses, which can be described by different averages. The most common averages are number average molar mass (M_n), weight average molar mass (M_w) and z-average molar mass (M_z) (Eq. 3–5). The polydispersity index (I) is calculated by dividing the weight average molar mass by the number average molar mass ($I=M_w/M_n$) and reflects the degree of heterogeneity in the molar mass distribution of the sample (Harding et al., 1991). For a polydisperse sample where I >1, a value of up to 1.1 reflects a sample that has a narrow distribution of molar mass and is therefore somewhat homogeneous. In practice this is only observed for fractionated polymers. Natural polysaccharides generally exhibit a polydispersity index of 1.6–2, but higher values can be observed.

$$M_n = \frac{\sum n_i M_i}{\sum n_i} \quad \text{(Equation 3)}$$

$$M_w = \frac{\sum n_i M_i^2}{\sum n_i M_i} \quad \text{(Equation 4)}$$

$$M_z = \frac{\sum n_i M_i^3}{\sum n_i M_i^2} \quad \text{(Equation 5)}$$

For obtaining molar mass data, there are several absolute methods, including those based on sedimentation equilibrium, osmotic pressure and light scattering techniques,

as reviewed by Harding et al. (1991). Sedimentation equilibrium is used in ultacentrifugation methods, where a concentration gradient of the solute is obtained through both sedimentation and diffusion (Cole et al., 2008). Osmotic pressure can be used for calculating M_n values, since the method is sensitive to the number of molecules in a dilute solution (Harding et al., 1991). M_w data can be obtained using static light scattering by directing a beam of light towards the polysaccharide chain and measuring the scattered light, which is proportional to the weight average molar mass of the molecule. In addition to these absolute methods, there are relative methods that require information or assumption on the conformation of the molecule or the use of calibration.

2.3.2.1 Size exclusion chromatography

Size exclusion chromatography (SEC), also known as gel permeation chromatography (GPC) or gel filtration chromatography (GFC), is a method where the separation of analytes is based on differences in hydrodynamic volume. The column is packed with a porous spherical material of a specific pore size, and the differences in migration velocity of the molecules, which depends on their size, determines the elution order (Barth, 1998; Striegel et al., 2009). The mobile phase flows through the column, accessing the pores of the packing material and spaces in between. The size of the analytes determines whether they can access the pores or only pass between them, creating differences in the migration rate. Molecules with a smaller hydrodynamic volume enter the pores and have a longer migration route through the packed column, and will have higher retention volume than larger molecules.

When optimising SEC retention, the flow rate and temperature have little effect, whereas the solvent and polymer branching have a certain influence (Striegel et al., 2009). For optimal separation, interaction between the analyte and the column packing material should be avoided. In SEC, also shear degradation and shearing of aggregated molecules can occur. Barth and Carlin (1984) reviewed shear degradation mechanisms in SEC analysis and suggested that shear degradation can occur in the injection valve, capillary tubes, column frits or packed column.

Shear rates are influenced by the flow rate and the diameter of the column packing material. Developments in the packing materials enabling the use of high pressures in the SEC system have led to modern high performance size exclusion chromatography (HPSEC) methods offering 10-fold better performance over conventional methods (Striegel et al., 2009). However, since shear rates in high performance systems are significantly greater than in conventional ones, the possibility of shear degradation should be considered (Barth and Carlin, 1984). Barth and Carlin (1984) compared shear rates caused by the column packing material in modern HPSEC and conventional SEC with flow rates of 1 ml/min, and reported about

20-fold difference. Interestingly, in HPSEC the most significant cause of shearing was found to be the capillary tubings, whereas these played a lesser role in conventional SEC. When considering shearing in HPSEC analysis, it should be noted that shear degradation is not necessarily easily distinquished from shear disaggregation. Maina et al. (2014) compared HPSEC and asymmetrical flow field-flow fractionation in the analysis of molar masses of dextrans and suggested that the observed differences in molar masses with these two methods were likely caused by disruption of aggregates in HPSEC, rather than actual shear degradation.

In SEC, the retention volume is proportional to the hydrodynamic size (or volume) of the analyte, not the molar mass directly (Gooding and Regnier, 2002). In order to transform the retention volume and detector output into molar mass data, calibration is needed unless the system is coupled with molar mass-sensitive detectors such as LS (Barth, 1998; Striegel et al., 2009). Since the retention volume is dependent on the hydrodynamic volume of the molecule, as well as on the pore dimensions of the column packing material, the calibration is only valid for a specific solvent-polymer combination in specific experimental conditions. The calibration can be done with a standard curve obtained using narrow molar mass distribution standards (Barth, 1998). The highest accuracy is obtained with standards that are structurally similar to the analysed molecules and that have low polydispersity. In aqueous systems, pullulan, poly(styrene sulfonate), poly(ethylene oxide) and poly(methacrylic acid) are commonly used as standards in this so-called primary calibration, while polystyrene, poly(methyl methacrylate), polyisoprene and polybutadiene are generally used with organic solvents. However, often standards that are structurally similar to the analyte with low polydispersity are not available, in which case secondary calibration is required. The calibration standards used in this case are similar to those for primary calibration, but the outcome should be considered an apparent molar mass distribution. Apparent molar mass distributions can be used e.g. for determining relative changes in molar mass distributions. Universal calibration is a method for establishing the relationship between molar mass and retention volume, when the relationship between molar mass and intrinsic viscosity is known (Giddings, 1994). The hydrodynamic volume (V_h) of the molecule can be calculated from the molar mass (M) and intrinsic viscosity ($[\eta]$), as shown in Eq. 6. The $[\eta]$ value can be determined when the system includes both a viscometer and concentration-sensitive detector.

$$[\eta] \propto \frac{V_h}{M} \qquad \text{(Equation 6)}$$

In addition to the calibration methods mentioned above, the detection of molar mass distribution can also be done with simultaneous use of both a light scattering detector and a concentration-sensitive detector. In this absolute detection system, the concentration of each molar mass fraction (at different retention volumes) is

measured, and the chromatographic slices are narrow enough to be able to assume that the molecules in one slice are monodisperse (Striegel et al., 2009). The molar mass is calculated for each chromatographic slice according to Eq. 7, where (LS) is the intensity of the light scattering signal (Eq. 8) and (RI) is the refractive index signal (Eq. 9) (Wen et al., 1996). K' can be calculated when the refractive index increment (*dn/dc*) and calibration constants for both LS (K_{LS}) and RI detectors (K_{RI}) are known (Eq. 10). The molar mass distribution (M_w, M_n) is then calculated using Eqs. 3 and 4, selecting appropriate sections of the chromatogram.

$$M = K' \times \frac{(LS)}{(RI)} \quad \text{(Equation 7)}$$

$$(LS) = K_{LS} c M (dn/dc)^2 \quad \text{(Equation 8)}$$

$$(RI) = K_{RI} c (dn/dc) \quad \text{(Equation 9)}$$

$$K' = \frac{K_{RI}}{K_{LS} \times dn/dc} \quad \text{(Equation 10)}$$

In SEC instrumentation, commonly used concentration-sensitive detectors are a refractive index (RI) detector and UV/Vis spectrophotometric detector. The UV/Vis detector is applicable only if the sample absorbs at UV or Vis wavelengths, and thus its use is more limited than the use of RI detector (Myers et al., 2000). In a basic RI detector, light is directed through the sample and separately through a reference cell and the passed light is detected with photodiodes (Striegel et al., 2009). If the refractive indices of the sample and reference differ, this results in a voltage difference between the photodiodes, which is seen as a signal. The response of the RI detector is dependent on the concentration but is mainly independent of the molar mass (Myers et al., 2000).

In molar mass analysis, static light scattering (SLS) detection may be used to obtain information about the molar mass and radius of gyration. In SLS techniques, a beam of light (often laser) is directed at the sample, and the scattered light is detected at different angles depending on the detection system. The resulting information is used to calculate the molar mass and radius of gyration (g_r). SLS techniques include low-angle light scattering (LALS), right-angle light scattering (RALS) and multi-angle light scattering (MALS). If the analysed molecules are small enough compared to the wavelength (<λ/20), the molar mass can be obtained with only one scattering angle, usually RALS detection measuring scattering at 90° (Harding and Jumel, 2001; Striegel et al., 2009). For molecules larger than λ/20, the scattering intensity depends

on the scattering angle and a zero-angle scattering value is required to get the molar mass data (Christensen et al., 2001; Harding and Jumel, 2001; Striegel et al., 2009). LALS can be used for this purpose, since its detection angle (<8°) is considered to be equivalent to zero. In MALS techniques, the scattering is detected at different angles and the data is extrapolated to the zero angle.

2.3.2.2 Field-flow fractionation

Field-flow fractionation (FFF) is a family of methods that are essentially flow-based separation methods. Instead of a column with stationary and mobile phases as in liquid chromatography, in FFF the analytes are separated according to size in a channel where no stationary phase or packing material is needed. The flow profile in the channel is parabolic, meaning that the velocity of flow is zero at the walls and increases with distance from the walls, being highest in the centre of the channel (Giddings, 2000). In parabolic flow without an applied field, the separation of macromolecules is minimal. In FFF methods a field is applied to separate the molecules by causing differences in their migration through the channel, leading to varying elution velocities.

FFF methods can be classified by the type of applied field. In sedimentation FFF, large particles (approx. 0.05–100 µm) are separated in a sedimentation field usually generated by centrifugal or gravitational forces (Giddings, 2000). Another field type is a temperature gradient field, which is used in thermal FFF. This is appropriate for polymers with molar masses of 10^4–10^7 g/mol. The third method, flow field-flow fractionation, uses a field created by a crossflow that is perpendicular to the main channel flow. Flow FFF (FlFFF), including symmetrical and asymmetrical FlFFF, is considered suitable for the broadest variety of molecules and particles (sizes ranging from approx. 0.001 to 50 µm or even 100 µm). Both thermal FFF and flow FFF have higher selectivity than SEC.

Asymmetrical flow field-flow fractionation (AsFlFFF) differs from symmetrical FlFFF in terms of the channel structure. In symmetrical FlFFF, both walls of the channel are porous frits and the cross-flow is generated using an external pump, which pushes liquid through the depletion wall (Yohannes, 2007; Wahlund, 2000). The same volume of liquid is drawn from the channel through the other wall, which is so-called accumulation wall. The accumulation wall is covered with a membrane, with a molar mass cut-off selected according to the sample size to allow flow-through of the eluent but not the analytes (Ratanathanawongs-Williams, 2000). In AsFlFFF the channel structure is otherwise similar, but only the accumulation wall is porous. The other wall is impermeable and the cross-flow is created only by the pressure difference between the channel and the space outside the permeable accumulation wall (Wahlund, 2000).

AsFlFFF involves different steps during analysis including injection, focusing, elution and rinsing (Wahlund, 2000). When the sample is injected into the channel, focusing flows are used to focus the molecules to a certain point at the accumulation wall. After the focusing step, the analytes start diffusing towards the centre of the channel, the differences in their diffusion coefficients leading to separation of the molecules (Fig. 5). Molecules that diffuse quickly end up in the centre of the channel, where the flow is fastest, and will elute first. A cross-flow resists the diffusion, and cross-flow rate gradients are used to enhance separation of the analytes.

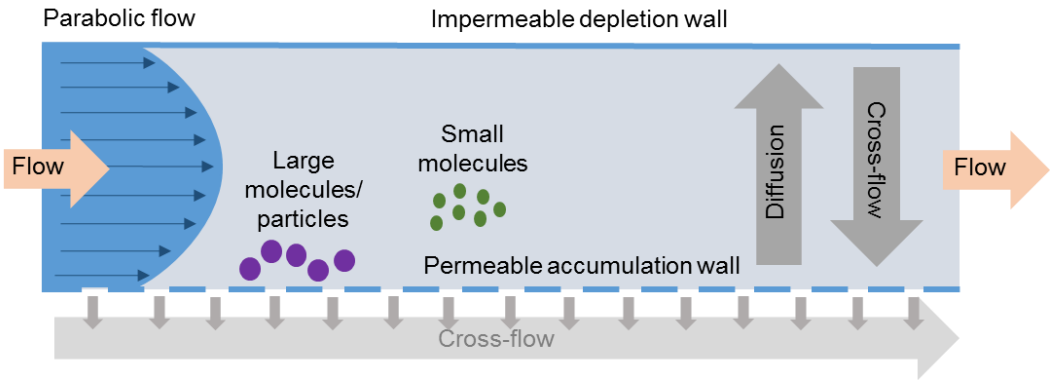

Figure 5. Separation of molecules/particles according to size in asymmetrical flow field-flow fractionation (AsFlFFF).

From the channel, the separated molecules continue to the detectors. Detectors that can be combined with AsFlFFF are similar to those used with HPSEC, i.e. viscometric, spectrophotometric, refractive index, and light scattering detectors (Myers et al., 2000). Similarly to HPSEC, to obtain the molar mass distribution a combination of a concentration-sensitive detector and a detector for molar mass or size is needed, if calibration with standards is not used.

3 Aims of the study

The main objective of the study was to investigate the oxidation pathways of cereal β-glucans and the consequent changes in the β-glucan structure and physicochemical properties. The study aimed additionally to link the structural information to the potential changes in rheological properties, which are known to be essential for both the technological and physiological functionality of β-glucans.

The more specific aims were:

1. To compare different oxidants and their efficacy in oxidising cereal β-glucans (I, II, IV)
2. To study the oxidation pathways of β-glucans and the products that are formed in oxidation (I, II)
3. To investigate physicochemical properties (e.g. aggregation and gelation) of native and oxidised cereal β-glucans and link the information to the oxidation status and the studied structural changes of β-glucans. (I, II, III).

4 Materials and methods

4.1 Materials

4.1.1 Materials for sample preparation

Commercial purified barley and oat β-glucans (BBG and OBG, respectively) were used. High viscosity BBG (Purity >94% and molar mass = 495 000 g/mol, reported by the manufacturer) and high viscosity OBG (Purity >94% and molar mass = 361 000 g/mol, reported by the manufacturer) were purchased from Megazyme (Ireland).

Oxidation reactions were initiated with hydrogen peroxide (H_2O_2, 30%, Merck, Germany), with L(+)-ascorbic acid (AA, J.T. Baker, Avantor Performance Material, USA or AnalaR NORMAPUR®, VWR Chemicals, Belgium) or with oxidised lipids including purified rapeseed oil (purification according to Lampi et al. (1999) to reach <1 µg/g of α- and γ-tocopherols) or methyl linoleate (ML, Nu Check Prep. Inc., MN, USA, purity >99%). All oxidations were catalysed with iron(II) sulphate heptahydrate ($FeSO_4 \times 7H_2O$) (Merck, Germany). In oxidations with oxidised lipids, polyoxyethylene sorbitan monolaurate (Tween20, Merck-Schuchardt, Germany) was used as an emulsifier.

Phytate removal was done using ion exchange resin (Amberlite® IRA-410 chloride form, 20–25 mesh, Sigma-Aldrich, MO, USA). The water used in all the studies, was Milli-Q grade.

4.1.2 Materials for analysis

Lithium bromide (LiBr), lithium chloride (LiCl), dimethyl sulfoxide (DMSO, HPLC grade), dimethyl acetamide (DMAc) and sodium nitrate ($NaNO_3$) were used in HPSEC and AsFlFFF analyses. Pullulan (molar mass = 788 000 g/mol, Polymer Laboratories, UK) was used for evaluation of detector performance in AsFlFFF. In HPSEC, the combined LS and viscometry and RI detectors were calibrated using the pullulan narrow standard (M_w = 212 000 g/mol). Carbonyl groups in β-glucan structures were labelled with carbazole-9-carbonyloxyamine (CCOA) and the labelled samples were analysed in HPSEC in LiCl/DMAc using cellulose standards with known carbonyl group contents (Potthast et al., 2015). For monosaccharide analysis, the samples were enzymatically hydrolysed using lichenase (endo-(1-3)(1-4)-β-D-glucan 4-glucanohydrolase, Megazyme, Ireland) and β-glucosidase (Megazyme, Ireland).

The oxidation status of lipids in study IV was monitored with the peroxide value, using ammonium thiocyanate (NH_4SCN), 96% ethanol, iron(II) chloride ($FeCl_2$), iron(III) chloride ($FeCl_3$, 10000 mg/l HCl) and hydrochloric acid (HCl).

4.2 Sample preparation

4.2.1 Dissolution of β-glucan

For studies I, II and IV, 0.7% (w/v) β-glucan solutions were prepared. Barley and oat β-glucans (BBG and OBG, respectively) were dissolved in volumetric flasks by wetting the purified β-glucan with 99.5% ethanol prior to dissolution with Milli-Q water. The samples were stirred at 85°C for 2 h using a magnetic stirrer. The samples were allowed to cool down and the flask was filled to the mark with Milli-Q water prior to continuing the stirring for an hour at room temperature.

In study III, BBG and OBG solutions were prepared as 1.250% and 1.875% (w/w), respectively. The dry samples were wetted with 99.5% ethanol and Milli-Q water was added by weighing the appropriate amount. Both OBG and BBG solutions were stirred for 2 h at three different temperatures: 37°C, 57°C and 85°C. The samples were allowed to cool down and the evaporated water was compensated by weighing the appropriate amount of Milli-Q water. Stirring was continued for 1 h at room temperature.

4.2.2 Oxidation of β-glucan solutions

4.2.2.1 Oxidation initiated by hydroxyl radicals (I, II, III)

Oxidation was initiated with H_2O_2 or AA, and $FeSO_4 \times 7H_2O$ was used as a catalyst in all the oxidations. The concentration of oxidant (H_2O_2 or AA) was 10 mM, 40 mM or 70 mM, and the concentration of $FeSO_4 \times 7H_2O$ was 1 mM in all the studies. After addition of the oxidising reagents, Milli-Q water was added to reach a β-glucan concentration of 0.56% (w/v) in studies I and II. In study III, the final BBG and OBG concentration was adjusted to 1% and 1.5% (w/w), respectively. In all the studies, a non-oxidised control sample diluted to the same concentration using Milli-Q water was used for comparison.

4.2.2.2 Lipid radical-mediated oxidation (IV)

Oxidation of BBG was initiated by addition of oxidised lipids. Purified rapeseed oil was stored in heptane (0.29 g/ml) and the heptane was evaporated with nitrogen flow prior to use. 6% oil-in-water (o/w) emulsions of both rapeseed oil and ML were prepared using 0.6% Tween20 as an emulsifier. These stock emulsions were made by ultrasonication (Labsonic U Braun, PA, USA) for 5 min, and the emulsions were kept cool in an ice bath during treatment. To produce oxidised stock emulsions containing hydroperoxides (LOOH), rapeseed oil and ML were oxidised in open containers at 55°C for 6 days prior to the preparation of stock emulsions. Additionally, ML was oxidised in conditions with limited oxygen to produce mildly-oxidised methyl linoleate.

The oxidation of β-glucan was studied by mixing 0.7% BBG with stock solutions of non-oxidised rapeseed oil (nRO), oxidised rapeseed oil (RO), mildly-oxidised methyl linoleate (MML) and highly-oxidised methyl linoleate (HML). The final emulsions contained 0.56% BBG, 1% oil (nRO, RO, MML, or HML), 0.1% Tween20 and 1 mM $FeSO_4 \times 7H_2O$.

4.2.3 Phytate removal

Wang et al. (2017) studied the phytic acid contents in the same commercial purified BBG and OBG as those used in studies I–IV. They reported a relatively high phytic acid content for OBG, since the content was 12.3 mg/g compared to 0.4 mg/g in BBG. Phytate is known to have antioxidant activity due to its ability to complex metal ions and thus hinder their catalytic activity in oxidation reactions (Graf and Eaton, 1990). Hence, in the oxidation study of OBG, both native OBG and phytate-removed OBG (pOBG) were used to see the effect of phytate on oxidation.

Phytate removal was done according to Wang et al. (2017). Ion exchange resin was first activated by washing in the following order: 1 M HCl, Milli-Q water, 1 M NaOH, Milli-Q water, 1 M HCl, Milli-Q water, 1 M HCl. The pH of 0.3% (w/v) β-glucan solution was adjusted to 4 with 1 M HCl prior to mixing the β-glucan with resin. The mixture was stirred at 4°C for 2 h, after which the solution was filtered through a cotton cloth. The β-glucan-containing filtrate was dialysed against Milli-Q water overnight and the dialysed solution was freeze-dried. This freeze-dried sample was then used for sample preparation according to 4.2.1 and 4.2.2.1.

4.3 Methods

4.3.1 Molar mass distribution of β-glucan

4.3.1.1 High performance size exclusion chromatography (I, II, IV)

The molar mass distribution and molar mass averages (I, II, IV) were analysed on day 4 using 0.01 M LiBr/DMSO as eluent according to Maina et al. (2014). To properly dissolve the non-oxidised and oxidised β-glucan samples prior to HPSEC analysis, the samples were diluted to 1.6 mg/ml with the eluent and stored at room temperature overnight (I, II). The samples containing lipid emulsions were stored at -20°C. Before the analysis, the lipid emulsion-containing samples were melted, diluted to 2 mg/ml with the eluent and dissolved by heating at 85°C for 30 min (IV).

The HPSEC instrument had an integrated autosampler and pump module (GPCmax, Viscotek Corp., USA). Detection of the analytes was conducted using a combined light scattering (λ0 = 670 nm, scattering angles 7° and 90°) and viscometric detector (270 Dual Detector, Viscotek Corp.) and a refractive index (RI) detector (VE 3580, Viscotek Corp.). A LF-G (4.6 × 10 mm, Showa Denko, Japan) guard column and two LF-804 columns (8 × 300 mm, exclusion limit 2 × 106, Showa Denko, Japan) were used. A flow rate of 0.8 ml/min and inection volume of 100 µl were used. A *dn/dc* value of 0.062 ml/g was used, according to Qin et al. (2013).

Carbonyl content analysis with simultaneous molar mass analysis (II) was done with an HPSEC system including a fluorescence detector, according to Röhrling et al. (2002 a,b), with some modifications. The non-oxidised and oxidised BBG and OBG samples were precipitated on day 4 with ethanol to remove the oxidation reagents. The samples were centrifuged and washed twice with 99.5% ethanol prior to drying at room temperature. For carbonyl analysis both the samples and cellulose standards were labelled with CCOA.

The dried samples (10 mg) and standards (20 mg) were activated by wetting with Milli-Q and rinsed with 96% ethanol on filter paper. Suspensions were prepared by adding 1 ml of 0.9% LiCl in DMAc to the activated samples/standards, and the suspensions were shaken overnight at room temperature. 2 ml of 1.25 mg/ml CCOA in acetate buffer (pH 4) was added and the suspensions were shaken at 40°C for 7 days. After this labelling treatment, the samples were centrifuged and the precipitates were dissolved with the eluent (0.9% LiCl in DMAc).

The HPSEC system consisted of a degasser (Dionex DG-2410, Thermo Scientific, USA), an autosampler (1100, Agilent, Germany), a pulse damper pump, a column

oven (25°C, STH 585, Gynkotek, Germany) and multiple detectors. A fluorescence detector (FL3000, Thermo Scientific, USA) was used for detecting the CCOA label (λ_{ex} = 290 nm and λ_{em} = 340 nm). For molar mass distribution, a multi-angle light scattering (MALS) detector (Wyatt Dawn DSP, Wyatt Technology, USA) with an argon ion laser (λ0 = 488 nm), and a refractive index (RI) detector (Shodex RI-71, Japan) were used. The system included four serial PLgel-mixed ALS (7.5 x 300 mm) columns (Agilent, Germany). 0.9% (w/v) LiCl in DMAc was used as eluent and the flow rate was 1.0 ml/min. A 100 µl injection volume and the *dn/dc* value of 0.136 were used. The MALS data was evaluated using Astra software (Wyatt Technology, USA) with a first-order Zimm fit. Additionally, Chromeleon and GRAMS/32 software (Thermo Scientific, USA) were used for analysing the carbonyl group content data.

The method gave the total amount of carbonyl groups, $c(C{=}O)_{tot}$, in the samples. Additionally, the equivalent amount of reducing end groups, $c(C{=}O)_{reg}$, was determined according to Eq. 11 from the number average molar mass (M_n).

$$c(C{=}O)_{reg} = \frac{1}{M_n} \times 10^6 \ \mu\mathrm{mol/g} \qquad \text{(Equation 11)}$$

4.3.1.2 Asymmetrical flow field-flow fractionation (I)

The AsFlFFF analysis of oxidised and non-oxidised samples was carried out in 0.1 M $NaNO_3$ and the sample solutions (5.6 mg/ml) were diluted to 1.6 mg/ml for analysis. Pullulan was analysed within each AsFlFFF run as an in-house reference to evaluate the performance of the system. The standard solution of 2 mg/ml was prepared by dissolving pullulan in 0.1 M $NaNO_3$ and the solution was kept at room temperature for 4 days to allow proper dissolution.

The AsFlFFF analyses were conducted using an AF2000 MT instrument (Postnova Analytics, Germany) coupled with two isocratic pumps, a piston pump and MALS (Brookhaven Instruments Corporation, USA) and RI (PN 3150, Postnova Analytics) detectors. The MALS detector had a 30 mW laser (λ0 = 660 nm) and seven scattering angles (35°, 50°, 75°, 90°, 105°, 130° and 145°). The 35° angle had a low signal-to-noise ratio, and was therefore excluded when analysing the data. The detectors were calibrated according to the instructions of the manufacturer. Separation occurred in a channel comprising a bottom plate with a ceramic frit, a spacer (thickness 350 µm) and a top plate to which the flow outputs were attached. In this study, two different membranes were used to cover the ceramic frit. A regenerated cellulose (RC) membrane with cut-off value of 10 000 g/mol and a polyethersulfone (PES) membrane with cut-off value of 1 000 g/mol were used depending on the molar mass of the sample.

The AsFlFFF analysis program involved several steps. The focusing step had a 7-min injection time with an injection flow rate of 0.2 ml/min and cross-flow of 1.0 ml/min. A cross-flow of 1.0 ml/min was also used at the start of the run and decayed exponentially (exponent 0.3). The flow rate to the detectors was constant at 0.5 ml/min and a SLOT flow of 0.5 ml/min to remove excess eluent from the upper part of the channel was used to intensify the signals. The Berry equation was used for data analysis. A *dn/dc* value of 0.146 ml/g was used according to Li et al. (2011).

4.3.2 Formic acid analysis (II)

The identification of formic acid was confirmed with nuclear magnetic resonance (NMR) spectroscopy using BBG oxidised with 70 mM H_2O_2/AA and 1 mM $FeSO_4 \times 7H_2O$ (study II). The formic acid (FA) content of non-oxidised and oxidised samples was measured using Formic acid assay (Megazyme, Ireland). The assay includes addition of formate dehydrogenase (FDH) and NAD^+ to the sample, and the formation of NADH in reaction 11 is followed spectrophotometrically.

$$FA + NAD^+ \xrightarrow{FDH} CO_2 + NADH + H^+ \qquad \text{(Reaction 11)}$$

The samples were prepared according to the assay instructions. An appropriate amount of 0.1 M NaOH was added to the samples to neutralise the oxidised samples, and an equal volume of Milli-Q water was added to the non-oxidised samples. The initial absorbances (A1) were measured at 340 nm, after which FDH was added to the samples and blanks. The final absorbances (A2) were measured at the end of the reaction (12 min). The absorbance differences ΔA (A2-A1) of the blank and the samples were calculated and ΔA_{blank} was subtracted from ΔA_{sample} to obtain $\Delta A_{formic\ acid}$. The formic acid contents (g/l) of the non-oxidised and oxidised samples were calculated using Eq. 12, where V is the final volume (ml), M is the molar mass of formic acid (g/mol), ε is the extinction coefficient of NADH at 340 nm, d is the light path (cm), and v is the sample volume (ml). The results were finally calculated as mg/g of β-glucan after taking the dilution into account.

$$c\left(\frac{g}{l}\right) = \frac{V \times M}{\varepsilon \times d \times v} \times \Delta A_{formic\ acid} \qquad \text{(Equation 12)}$$

As explained above, the analysis is based on measurement of NADH, which is formed in Reaction 11. Thus, AA was assumed to cause some error in the measurement, since it can act as a reducing agent. For this reason, the effect of AA was tested with reagent blank samples. These test samples contained the same amount of AA and $FeSO_4 \times 7H_2O$ as the actual oxidised β-glucan samples. The results of these reagent blanks were subtracted from the results of the BBG and OBG samples oxidised with AA.

4.3.3 Monosaccharide analysis (II)

4.3.3.1 Sample preparation

For the analysis of glucose and arabinose, the samples were enzymatically hydrolysed to monosaccharides. The hydrolysis of non-oxidised and oxidised BBG and OBG samples (5.6 mg/ml) was conducted by adding 60 µl of 50 U/ml lichenase and 40 µl of 2 U/ml β-glucosidase to 200 µl of sample. The concentration of the sample was simultaneously adjusted to 2.8 mg/ml with Milli-Q water. Samples were then incubated for 24 h at 40°C prior to inactivation of the enzymes by boiling for 10 min. The samples were stored at -20°C prior to the monosaccharide analysis.

Appropriate dilutions of the samples were done for the monosaccharide analysis. Glucose and arabinose standards in the concentration range 0.005–0.200 mg/ml and 0.002–0.100 mg/ml, respectively, were used. Deoxygalactose was used as an internal standard in all the standards and samples. The glucose and arabinose contents were reported as a percentage of the total theoretical glucose amount in the native non-oxidised sample. The amount of arabinose was analysed to see whether formation of arabinose occurred due to oxidation reactions of β-glucan.

4.3.3.2 Monosaccharide analysis using high performance anion exchange chromatography with pulsed amperometric detection

Glucose and arabinose analysis was conducted with HPAEC-PAD according to Johansson et al. (2006), with some modifications. The system included an autosampler (Waters 2707, USA), two SSI pulse equalisers (model LP 21, Scientific systems Inc, USA), three pumps (Waters 515 HPLC pumps, USA) and a pulsed amperometric detector (Waters 2465, USA). A CarboPac PA-1 guard column (50×4 mm, Dionex Corporation, USA) and CarboPac PA-1 analytical column (250×4 mm, Dionex Corporation, USA) were used at 30°C. The flow rate was set to 1 ml/min and a gradient of two eluents, 200 mM NaOH (A) and Milli-Q water (B), was used in addition to post-column addition of 300 mM NaOH using a 0.3 ml/min flow rate. The eluent ratio A:B ranged from 1:99 to 100:0 during the run. The detection was conducted at 30°C using the following pulse potentials and durations: $E1$ = 0.05 V, $t1$ = 400 ms, $E2$ = 0.75 V, $t2$ = 120 ms, $E3$ = -0.80 V, $t3$ = 130 ms, ts = 20 ms. Empower 3 software (Waters, USA) was used for data processing.

4.3.4 Rheological measurements

4.3.4.1 Rotational measurement (III, IV)

The viscosities of the samples were measured at 20°C with a rheometer (Haake RheoStress 600, Thermo Electron GmbH, Germany). A cone and plate geometry with either 35 mm diameter and 2° cone angle (III) or 60 mm diameter and 1° cone angle (IV) was used. A stepwise rotation program with a shear rate ranging from 1 to 100 s^{-1} and 100 to 1 s^{-1} was used for all the samples. The viscosities were compared at either 14 s^{-1} (III) or 10 s^{-1} (IV).

4.3.4.2 Oscillatory measurement (III)

The storage (G') and loss (G'') moduli were measured at 20°C with a rheometer (Haake RheoStress 600, Thermo Electron GmbH, Germany). A parallel plate and plate geometry with a diameter of 35 mm was used. The oscillation frequency ranged from 0.01 to 10 Hz and the strain was 0.4 in all the measurements, after ensuring with a strain sweep that the analysis was carried out within the linear viscoelastic range of the samples.

4.3.5 Analysis of lipid oxidation extent

4.3.5.1 Peroxide value measurement

The peroxide value (PV) measurement was conducted according to Ueda et al. (1986). Appropriate dilutions of samples were done prior to measurement. 200 µl of 30% (w/v) aqueous solution of NH_4SCN and 10 ml of 96% (v/v) ethanol were mixed prior to addition of 200 µl of the sample solution. The first absorbance was measured at 500 nm 3 min after addition of 200 µl of 20 mM $FeCl_2$ in 3.5% HCl. Samples containing β-glucan had some precipitate due to the ethanol in the solution, and were thus filtered prior to measurement. A standard curve of 0–40 µg of $FeCl_3$ was prepared.

Eq. 13 was used to calculate the *PV* (mequiv peroxide/kg of sample). A_{sample} is the absorbance of the measured sample, A_{blank} is the absorbance of the blank sample, *b* is the y-axis intercept, *k* is the slope of the standard curve, 55.84 is the atomic weight of Fe, and m_{sample} is the mass of the sample in grams.

$$PV = \frac{\frac{\left(A_{sample} - A_{blank}\right) - b}{\mathrm{k}}}{55.84 \times m_{sample} \times 2} \qquad \text{(Equation 13)}$$

4.3.5.2 Hexanal content analysis

Headspace gas chromatography was used for hexanal analysis. The system included a GC instrument (Perkin Elmer, USA), an autosampler (Perkin Elmer HS 40XL), a Nordibond-54 column (25 m × 0.32 mm) and flame ionization detector (FID). 0.5 g of emulsion sample was weighed into the headspace vials. The samples were pre-heated in the autosampler for 10 min at 60°C, after which they were heated at 80°C for 18 min to allow the volatile compounds to equilibrate between the gas and liquid phases. A 2-min pressurisation with helium prior to injection to the column was used. The separation was conducted at 60°C and FID detection at 250°C. ChemStation GC software was used for data processing. The results are presented as hexanal peak areas. The stability of the system was evaluated by regularly injecting a hexanal standard to monitor the response of the detector.

4.4 Statistical analysis (I-IV)

Samples were prepared in three replicates. However, only two replicates were used for CCOA-labelling and HPSEC analysis of non-oxidised samples. All other analyses were done for all three replicates. The results were reported as average ± standard error of the mean (SEM).

Statistical analyses were performed with the Statistical Package for the Social Sciences (SPSS Statistics version 23/24, IBM, USA) using one-way analysis of variance (ANOVA) with a post-hoc Tukey test, except for study III where a post-hoc LSD test was used instead. A logarithmic transformation of the data was applied prior to statistical analysis if there were >10-fold differences in the values between the compared samples. Differences were considered significant at $P<0.05$.

5 Results

5.1 Macromolecular properties of non-oxidised and oxidised β-glucans (I, II, IV)

5.1.1 Molar masses of non-oxidised β-glucans (I)

Molar masses of native (non-oxidised) BBG and OBG were analysed with HPSEC in DMSO and with AsFlFFF in aqueous eluent, and the results of the two methods were compared (Table 1). HPSEC and AsFlFFF gave comparable M_w results for both BBG (520 000 g/mol and 550 000 g/mol, respectively) and OBG (420 000 g/mol and 400 000 g/mol, respectively), which were similar to those reported by the manufacturer: 495 000 g/mol for BBG and 361 000 g/mol for OBG. The polydispersity indices obtained from AsFlFFF analysis were somewhat higher than those obtained from HPSEC analysis. Recoveries were above 88% for all samples in both systems and relatively low SEM values were obtained. Generally, AsFlFFF gave lower SEM values than HPSEC.

Table 1. Weight average molar masses (M_w), number average molar masses (M_n), polydispersity indices (M_w/M_n) and recoveries of non-oxidised barley and oat β-glucan (BBG and OBG, respectively) analysed with high performance size exclusion chromatography (HPSEC) and asymmetrical flow field-flow fractionation (AsFlFFF). Results reported as average ± SEM.

System	Measured parameter	β-glucan samples		
		BBG	OBG[c]	pOBG[c, d]
HPSEC[a]	M_w (x10^3 g/mol)	520 ± 20	420 ± 30	n.a.
	M_n (x10^3 g/mol)	430 ± 20	300 ± 50	n.a.
	M_w/M_n	1.2 ± 0.0	1.4 ± 0.2	n.a.
	Recovery (%)	88 ± 2	92 ± 0	n.a.
AsFlFFF[b]	M_w (x10^3 g/mol)	550 ± 0	400 ± 10	570 ± 20
	M_n (x10^3 g/mol)	290 ± 10	210 ± 10	100 ± 50
	M_w/M_n	1.9 ± 0.0	1.9 ± 0.1	11 ± 6
	Recovery (%)	93 ± 1	89 ± 5	103 ± 0

[a]Measurements conducted on day 1 after diluting the samples with eluent and storing overnight.
[b]Measurements conducted on day 0
[c]Unpublished data.
[d]Phytate removed from OBG with ion exchange resin.
n.a. = not analysed

5.1.2 Changes in the macromolecular properties of β-glucan due to oxidation with various oxidants

5.1.2.1 Oxidation initiated by hydroxyl radicals (I, II)

Oxidation was initiated with H_2O_2 or AA using ferrous sulphate as a catalyst. Both oxidants were shown to cause degradation of β-glucan. The M_w values of the oxidised BBG were followed with AsFlFFF daily for 4 days to see whether the molar mass decreased constantly during the oxidation period. The effect of oxidation on M_w was shown to be highest during the first oxidation day, after which only slight (with 70 mM H_2O_2) or no decrease (10 mM H_2O_2 and 10 mM AA) in M_w was observed (Fig. 6). Figure 6 also shows that H_2O_2 oxidised BBG more than AA, since the molar mass decrease was significantly lower with AA.

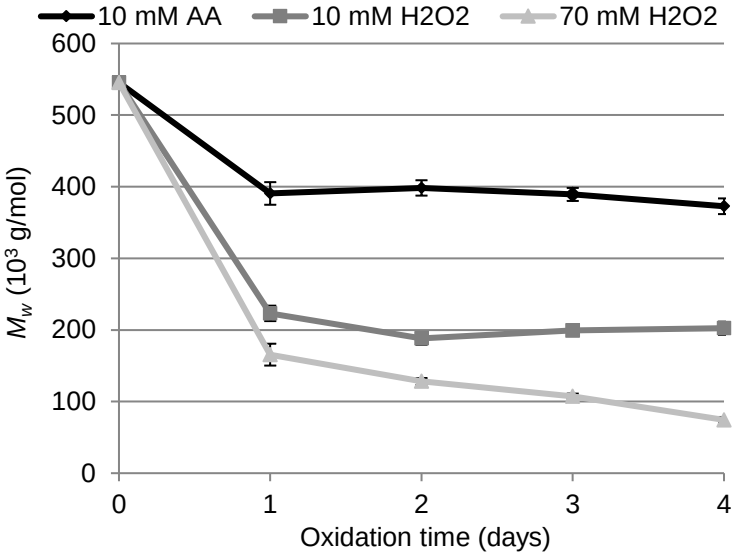

Figure 6. Decrease of weight average molar mass (M_w) of BBG as a function of oxidation time measured with AsFlFFF. 1 mM $FeSO_4 \times 7H_2O$ used as a catalyst in all oxidations. Figure adapted from study I.

To ensure that the variation in oxidation extent depending on the oxidant was not caused by differences in the acidity, the pH values of the samples were checked. The native BBG solution had a near-neutral pH (6.7), which decreased to 3.0–3.2 in each oxidised sample immediately after addition of both the catalyst and the oxidant. Thus, the pH was similar in both AA and H_2O_2 oxidised samples and the differences in oxidation were not due to the pH.

Comparison of HPSEC and AsFlFFF in analysis of molar masses of oxidised β-glucans

In AsFlFFF elugrams, for H_2O_2-oxidised β-glucans two peaks were separated and could be individually integrated, while HPSEC chromatograms showed only one broad peak. Table 2 shows the AsFlFFF results for the total sample and for the two peaks separately, LM and HM representing the peaks that eluted in the low and high molar mass area, respectively (Fig. 7). Most of the oxidised samples consisted of low molar mass products, with high molar mass products accounting for only a minor part. This was seen as a high signal in the LM area for the concentration-sensitive RI detector, indicating a large amount of smaller molecules, and also as s high signal in the HM area for the size-sensitive LS detector, indicating a lower amount of very large molecules. E.g. in BBG, OBG and phytate-removed OBG (pOBG) oxidised with 70 mM H_2O_2, the HM peak comprised only about 3%, 7% and 2% of the total integrated sample, respectively.

The M_w values of H_2O_2-oxidised β-glucans analysed with HPSEC were comparable to those of the LM peak in AsFlFFF analysis. Oxidation of BBG with 70 mM H_2O_2 resulted in a M_w of 71 000 g/mol and 74 000 g/mol, analysed with HPSEC and AsFlFFF, respectively (Table 2). For OBG samples oxidised for 4 days with 70 mM H_2O_2, the molar mass decreased less and the two methods gave similar M_w results: 200 000 g/mol with HPSEC and 230 000 g/mol with AsFlFFF. The HM peak of AsFlFFF consisted of really large molecules, which skewed the M_w when the total area was integrated. This kind of behaviour was not detected with HPSEC, and no separate peaks for different sizes of molecules were obtained.

Analysis of oxidative degradation

Since with AsFlFFF a better separation and larger distribution of molecular sizes were obtained, the oxidative degradation of β-glucan samples was more closely analysed from the AsFlFFF data. Oxidation with AA seemed to cause less degradation of β-glucans than with H_2O_2 (Table 2). According to the AsFlFFF analysis, 4 days of oxidation with 10 mM AA led to a 33% and 26% decrease in M_w of BBG and pOBG, respectively, but in OBG the molar mass was even higher after oxidation with AA (520 000 g/mol compared to 400 000 g/mol in non-oxidised OBG). However, in AA-oxidised samples only one broad peak eluted, and thus separate integration of single oxidised molecules and possible aggregates was not possible (elugram for BBG in Figure 8). M_w/M_n was also rather high for AA-oxidised OBG and pOBG (2.5 and 2.8, respectively) (Table 2).

Table 2. Weight average molar masses (M_w), polydispersity indices (M_w/M_n) and weight average radii of gyration (R_w) of oxidised BBG, OBG and pOBG. Samples oxidised for 4 days with 10 mM AA, 10 mM H_2O_2 and 70 mM H_2O_2 and 1 mM $FeSO_4 \times 7H_2O$ used as a catalyst in all oxidations.

			BBG			OBG[c]			pOBG[c, d]		
Method	Oxidant	Integrated area	M_w (x10^3 g/mol)	M_w/M_n	R_w (nm)	M_w (x10^3 g/mol)	M_w/M_n	R_w (nm)	M_w (x10^3 g/mol)	M_w/M_n	R_w (nm)
HPSEC	10 mM AA	Total area	260 ± 0	1.5 ± 0.0		230 ± 0	1.9 ± 0.2				
	10 mM H_2O_2	Total area	180 ± 10	1.5 ± 0.0		190 ± 10	1.4 ± 0.0				
	70 mM H_2O_2	Total area	71 ± 1	1.6 ± 0.1		200 ± 20	1.4 ± 0.1				
ASFlFFF	10 mM AA	Total area	370 ± 10	2.1 ± 1.0	34 ± 1	520 ± 10	2.5 ± 0.1	61 ± 1	420 ± 10	2.8 ± 0.1	38 ± 3
		Total area	5700 ± 200	69 ± 12	36 ± 3	4800 ± 300	35 ± 5	59 ± 3	4000 ± 100	71 ± 16	35 ± 3
	10 mM H_2O_2	HM peak[a]	160000 ± 10000	9.2 ± 1.6	69 ± 1	30000 ± 1000	9.0 ± 1.7	66 ± 0	25000 ± 2000	6.9 ± 0.5	64 ± 1
		LM peak[b]	200 ± 10	2.6 ± 0.4	35 ± 3	240 ± 10	2.0 ± 0.4	57 ± 3	150 ± 10	2.3 ± 0.4	30 ± 3
		Total area	4900 ± 100	130 ± 10	27 ± 2	3900 ± 100	32 ± 1	52 ± 2	400 ± 50	14 ± 2	34 ± 2
	70 mM H_2O_2	HM peak[a]	180000 ± 20000	7.4 ± 2.4	61 ± 1	54000 ± 1000	7.3 ± 0.3	61 ± 1	28000 ± 9000	440 ± 30	86 ± 8
		LM peak[b]	74 ± 4	2.0 ± 0.1	26 ± 2	230 ± 10	2.0 ± 0.0	51 ± 2	48 ± 2	1.6 ± 0.2	34 ± 1

[a]The peak eluting in the high molar mass area in the elugram is integrated.

[b]The peak eluting in the low molar mass area in the elugram is integrated.

[c]AsFlFFF results of OBG and pOBG are unpublished data.

[d]Phytate removed from OBG with ion exchange resin. These samples were stored frozen and heated at 85°C for 30 min to dissolve prior to analysis

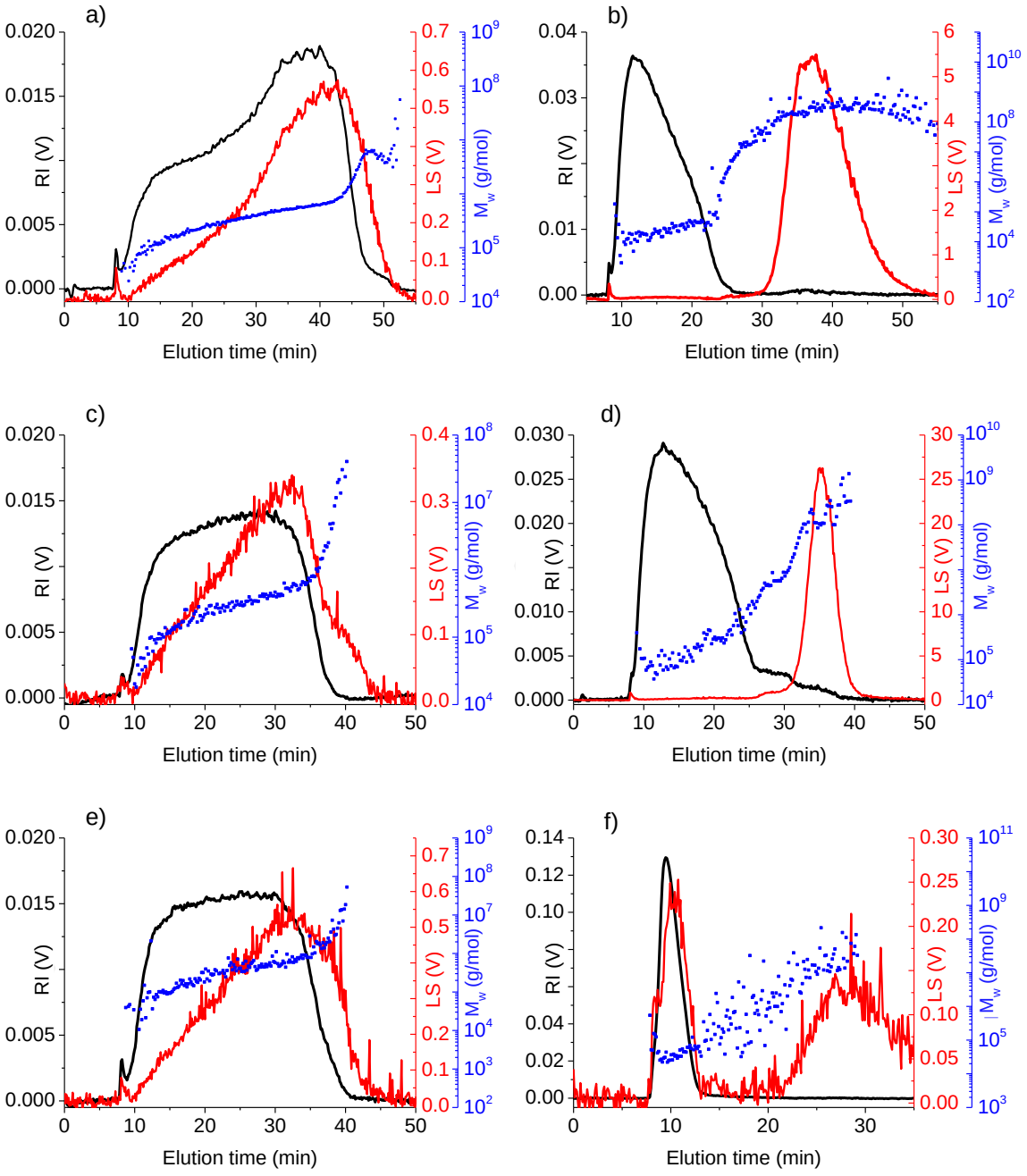

Figure 7. AsFlFFF elugrams of BBG (a, b), OBG (c, d) and pOBG (e, f) before (a, c, e) and after (b, d, f) oxidation for 4 days with 70 mM H_2O_2 using 1 mM $FeSO_4 \times 7H_2O$ as a catalyst.

In H_2O_2-oxidised β-glucan samples, more significant degradation was shown (Table 2). Oxidation with 10 mM H_2O_2 led to a 64%, 40% and 74% decrease in M_w of BBG, OBG and pOBG, respectively, when comparing M_w of the LM peak after 4 days of oxidation with M_w obtained for a non-oxidised sample. The oxidant concentration affected the oxidation of BBG and pOBG, since 70 mM H_2O_2 oxidised β-glucan even more efficiently than 10 mM H_2O_2, and resulted in a M_w decrease of 87%, 43% and 92% for BBG, OBG and pOBG, respectively. For OBG, which contained phytate, no

significant difference was seen between the two H_2O_2 concentrations. When comparing M_w of the HM peaks of different β-glucan samples, a higher M_w was shown for BBG compared to OBG and pOBG.

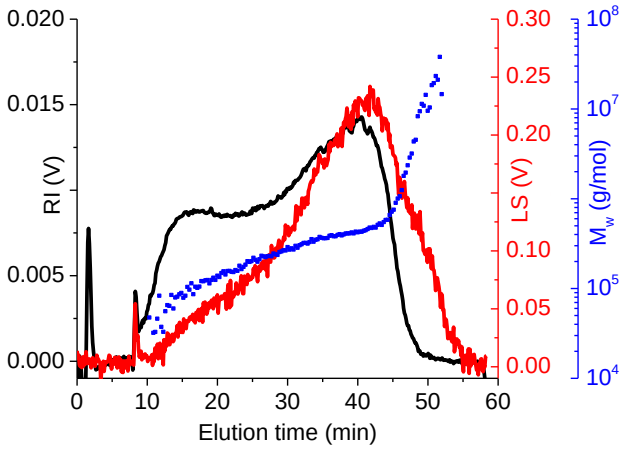

Figure 8. AsFlFFF elugram of BBG oxidised for 4 days with 10 mM AA and 1 mM $FeSO_4 \times 7H_2O$ as a catalyst.

5.1.2.2 Lipid radical-induced oxidation (IV)

Oxidation status of lipids analysed by peroxide value and hexanal content

The peroxide value was used to indicate the amount of primary lipid oxidation products, i.e. hydroperoxides. The peroxide values of emulsions containing β-glucan, ferrous iron and non-oxidised rapeseed oil (nRO), oxidised rapeseed oil (RO) or mildly-oxidised methyl linoleate (MML) all increased throughout the 7-day storage time (Fig. 2a in study IV). After 7-day storage, emulsions oxidised with nRO and RO had a peroxide value of 740 mequiv/kg and 670 mequiv/kg, respectively. In MML-containing emulsion, the peroxide value was 2 200 mequiv/kg, increasing somewhat evenly during storage (measured on day 0, 3 and 7). In emulsion oxidised with highly-oxidised methyl linoleate (HML), the trend was somewhat different, since the peroxide value was constantly high (1 500–1 600 mequiv/kg at all measurement points).

Hexanal is one of the secondary oxidation products of lipid oxidation resulting from the decomposition of hydroperoxides. The hexanal contents of the emulsions on day 0 were relatively low (hexanal peak area 0–6×10^4), but after 7-day oxidation the hexanal contents of emulsions oxidised with nRO, RO, MML and HML had increased around 6-fold, 2-fold, 2-fold and 8-fold, respectively (Fig. 2b in study IV). The large increase in the hexanal content of HML emulsion, while the hydroperoxide content remained stable, indicates that the decomposition of hydroperoxides occurred at the same rate as the formation of new ones

Changes in macromolecular properties of β-glucan due to lipid radical-induced oxidation

The oxidation of β-glucan was investigated by viscosity measurement and M_w analysis with HPSEC. The viscosity of the emulsions oxidised with nRO, RO, MML and HML decreased by 19%, 20%, 12% and 26%, respectively. M_w decreased by 28%, 21%, 26% and 46%, respectively (Table 2 in study IV). BBG in emulsion with the most oxidised lipid, HML, was shown to degrade the most, resulting in a M_w of 310 000 g/mol after 7 days of oxidation. For comparison, the viscosity of emulsion with BBG and Fe but without oil was also measured, and the viscosity of this control sample decreased by 6.5% during the 7-day storage time.

5.2 Oxidation pathways (II)

5.2.1 Formation of carbonyl groups due to oxidation of β-glucan

M_w decrease percentages of oxidised, precipitated and CCOA-labelled BBG and OBG samples are shown in Table 3. The M_w values of the labelled samples (analysed with HPSEC using 0.9% LiCl in DMAc as eluent) were compared to the non-labelled, fresh samples (analysed with HPSEC using 0.01 M LiBr in DMSO) to ensure that precipitation and labelling processes did not cause degradation. The methods gave comparable M_w values (data shown in study II). Thus, new reducing end carbonyls can be considered to result from oxidative degradation only.

CCOA-labelling labels both keto and aldehyde groups, and thus the total amount of carbonyls, $c(C=O)_{tot}$, includes both the reducing end carbonyls and carbonyls within the β-glucan chain. The concentration of reducing end carbonyls, $c(C=O)_{reg}$, can be calculated from the M_n value (Eq. 11), and comparing the $c(C=O)_{reg}$ value of the oxidised samples with the original $c(C=O)_{reg}$ value of the non-oxidised sample indicates the amount of new reducing end groups formed during oxidative degradation.

The total carbonyl contents increased in both BBG and OBG samples due to oxidation. The increase was more significant in H_2O_2-oxidised samples, 70 mM H_2O_2 leading to a 28-fold and 14-fold increase in BBG and OBG, respectively, but 70 mM AA only to a 4-fold and 2-fold increase. In AA-oxidised BBG and OBG, most of the carbonyl groups newly formed during oxidation were shown to be reducing end carbonyls (62% and 97% of the total carbonyl amount in BBG and OBG, respectively, oxidised with 70 mM AA). However, in H_2O_2-oxidised samples, most of the carbonyls were not reducing end carbonyls, since in samples oxidised with 70 mM H_2O_2,

reducing end carbonyls corresponded to only 36% and 21% of the total amount of carbonyls in BBG and OBG, respectively.

Table 3. Weight average molar mass (M_w) decreases and carbonyl contents of non-oxidised and oxidised BBG and OBG on day 4. Oxidation was initiated with different concentrations of H_2O_2 or AA, and 1 mM $FeSO_4 \times 7H_2O$ was used as a catalyst.

Sample	Treatment	M_w decrease[a, b] (%)	$c(C=O)_{tot}$ (µmol/g)[c]	$c(C=O)_{reg}$ (µmol/g)[d]
BBG	Non-oxidised		2.4	2.2
	10 mM H_2O_2	71	40	10
	40 mM H_2O_2	79	57	15
	70 mM H_2O_2	89	66	24
	10 mM AA	45	7	4.8
	40 mM AA	45	8.8	4.8
	70 mM AA	54	9.4	5.8
OBG	Non-oxidised		3.3	3.6
	10 mM H_2O_2	50	31	6.6
	40 mM H_2O_2	43	40	6.6
	70 mM H_2O_2	60	46	9.5
	10 mM AA	38	7.1	5.8
	40 mM AA	45	8	6.4
	70 mM AA	40	6.9	6.7

[a]Samples analysed after precipitation and CCOA-labelling with HPSEC in 0.9 % LiCl/DMAc.

[b]M_w of oxidised vs. non-oxidised sample, which was 560 000 g/mol for BBG and 400 000 g/mol for OBG.

[c]Total carbonyl content determined from CCOA-labelling.

[d]Calculated concentration of reducing end groups based on M_n values (not shown) of labelled samples using Eq. 11.

5.2.2 Formation of formic acid and arabinose

Formation of formic acid occurred in oxidised samples. The identification of formic acid was confirmed with NMR (Fig. 2 in study II) and the formic acid quantified spectrophotometrically. As shown in Fig. 9, the formic acid accumulated in BBG and OBG oxidised with H_2O_2 and its content increased with increasing oxidant concentration. The formic acid content was significantly higher in BBG samples than in OBG samples, e.g. 13.6 mg/g in BBG and 3.3 mg/g in OBG oxidised for 4 days with 70 mM H_2O_2. However, in all non-oxidised and AA-oxidised samples the formic acid contents were relatively low (<0.3 mg/g and ≤1.5 mg/g, respectively).

Simultaneously with formic acid, arabinose was also formed. Glucose contents were analysed to verify that they decreased when decomposition to arabinose was observed (data shown in study II) . Arabinose was not seen in other samples than those oxidised with H_2O_2, and in those the content was highly dependent on the H_2O_2 concentration. Interestingly, the arabinose content decreased from day 1 to day 4 in both BBG and OBG samples. On day 1, the arabinose contents of BBG and OBG oxidised with 70 mM H_2O_2 were 1.0% and 1.6%, respectively, but after 4 days of oxidation the contents were only 0.9% and 1.3%, respectively. It should be noted that although the formic acid contents were higher in BBG than in OBG, for arabinose the trend was different, since OBG had the highest arabinose contents.

5.3 Rheological properties of β-glucan in aqueous solutions (III)

5.3.1 Rheology of sufficiently dissolved β-glucan solutions

Based on study I, total dissolution of β-glucan was expected at 85°C. BBG85 and OBG85 were used as control samples in rheological experiments. Apparent viscosities of non-oxidised BBG85 (Fig. 10a) and OBG85 (Fig. 10b) were similar (290 mPa·s and 340 mPa·s, respectively, on day 7, measured at $14 s^{-1}$) and were shown to remain quite stable during the 7-day storage time (Table 4). However, the viscosities decreased significantly upon oxidation. After oxidation with 70 mM H_2O_2 for 1 day, there was a clear difference in the viscosity losses of BBG85 and OBG85; the viscosities had decreased to 16 mPa·s (viscosity loss 94%) and 71 mPa·s (viscosity loss 78%), respectively, measured at 14 s^{-1} (Table 4). After 7 days of oxidation, the viscosity losses were similar and resulted in viscosities of 6.4 mPa·s (viscosity loss 98%) and 20 mPa·s (viscosity loss 94%) in BBG85 and OBG85, respectively. No hysteresis was observed in either BBG85 (Fig. 10a) or OBG85 (Fig. 10b), and thus no structure formation (e.g. entanglements) was expected. Oscillatory measurements were not conducted, as there was no hysteresis.

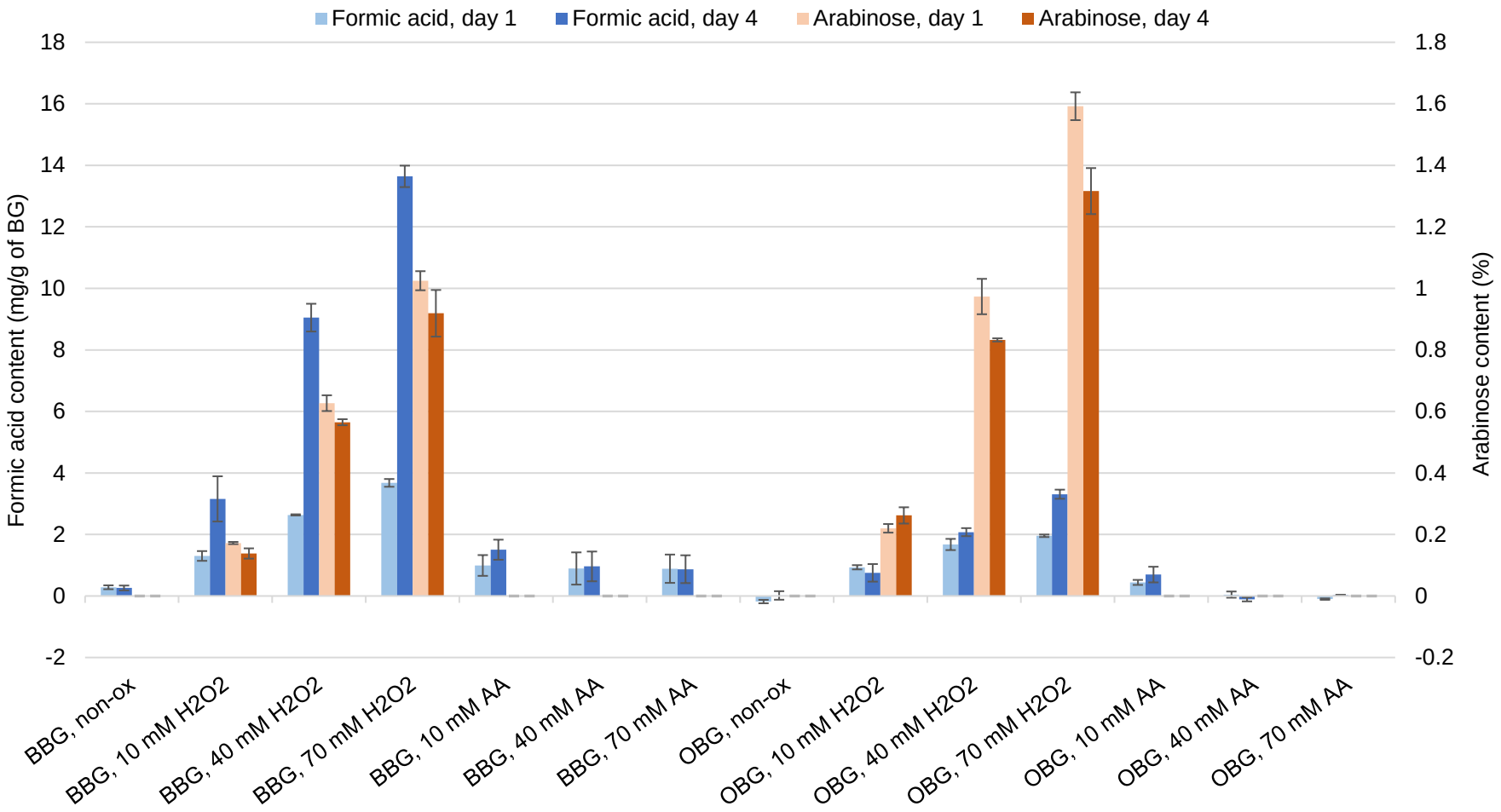

Figure 9. Formic acid and arabinose contents of non-oxidised (non-ox) and oxidised BBG and OBG samples on day 1 and day 4. Oxidation was initiated with different concentrations of H_2O_2 or AA, and 1 mM $FeSO_4 \times 7H_2O$ was used as a catalyst.

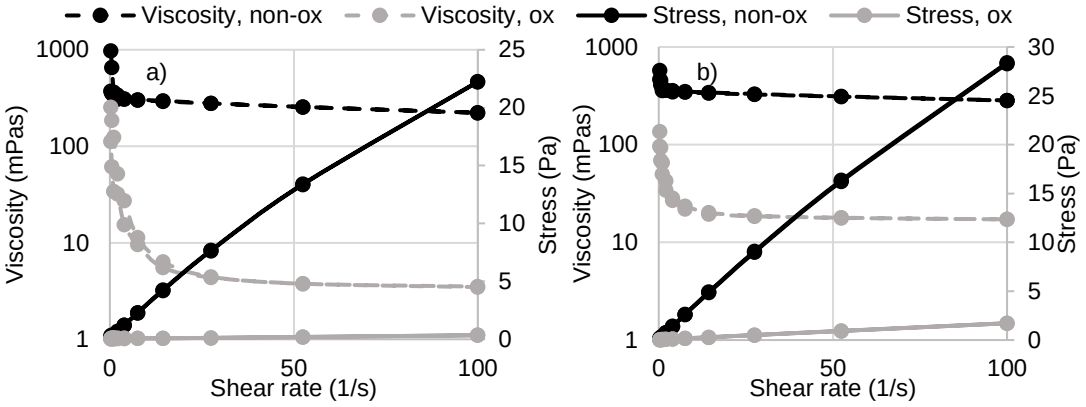

Figure 10. Viscosity and shear stress curves of non-oxidised (non-ox) and oxidised (ox) BBG85 (1.0%, w/w) (a) and OBG85 (1.5%, w/w) (b). Measurements were conducted with a rotational rheometer at 20°C using a cone-and-plate geometry on day 7. Oxidation was initiated with 70 mM H_2O_2 and 1 mM $FeSO_4 \times 7H_2O$.

Table 4. Viscosities of non-oxidised and oxidised BBG (1%, w/w) and OBG (1.5%, w/w) samples dissolved at different temperatures. Oxidation was initiated with 70 mM H_2O_2, and 1 mM $FeSO_4 \times 7H_2O$ was used as a catalyst. Adapted from study III.

Sample material	Dissolution temperature	Gelation time	Viscosity[a] (mPa·s)	
			Non-oxidised	Oxidised
BBG	37˚C	Day 1	1300 ± 900	2100 ± 400
		Day 4	1600 ± 600	1500 ± 500
		Day 7	810 ± 170	2000 ± 700
	57˚C	Day 1	530 ± 10	76 ± 18
		Day 4	740 ± 20	120 ± 20
		Day 7	770 ± 30	50 ± 2
	85˚C	Day 1	290 ± 10	16 ± 2
		Day 4	300 ± 10	6.7 ± 0.2
		Day 7	290 ± 10	6.4 ± 0.6
OBG	37˚C	Day 1	660 ± 60	340 ± 90
		Day 4	950 ± 90	840 ± 270
		Day 7	1400 ± 200	1000 ± 300
	57˚C	Day 1	360 ± 20	100 ± 10
		Day 4	390 ± 50	110 ± 10
		Day 7	440 ± 50	130 ± 20
	85˚C	Day 1	330 ± 0	71 ± 8
		Day 4	330 ± 10	30 ± 3
		Day 7	340 ± 10	20 ± 1

[a]Average viscosities at 14 s^{-1}.

5.3.2 Rheological properties of β-glucan dissolved at low temperatures

To understand the rheological properties of non-oxidised and oxidised samples, rotational and oscillatory measurements were carried out. For this study, low concentrations were used and the effect of dissolution temperature was evaluated.

5.3.2.1 Rotational measurements

Pre-tests showed two interesting dissolution temperature areas, which were chosen to be studied further. OBG was shown to be prone to structure formation at temperatures near the physiological temperature, since dissolution temperatures from 35°C to 45°C all led to some gel structure formation. For BBG, the dissolution temperature area leading to gelation was rather narrow, with 57°C leading to gelation but not 55°C or 60°C. Thus, in addition to 85°C, which was used as a control temperature with proper dissolution, two lower dissolution temperatures were chosen according to the pre-tests to be 37°C (physiological temperature) and 57°C.

In BBG37, the viscosity of non-oxidised and oxidised samples varied between the time points, but additionally the deviation was high (Table 4). Stress curves showed large hysteresis loops (Fig. 11a), suggesting some structure formation. However, the structure of non-oxidised and oxidised BBG37 was heterogeneous and the samples contained visible particles, which probably caused disturbances in the rheological measurements. Oscillation of BBG37 samples was not conducted, as the sample structure was clearly not gel-like. Thus the observed hysteresis loop was not caused by gelation but by the particles in the sample.

The viscosities of non-oxidised and oxidised OBG37 were significantly higher than those of OBG85 (1 400 mPa·s and 1 000 mPa·s for OBG37, respectively, and 340 mPa·s and 20 mPa·s for OBG85, measured on day 7 at 14 s^{-1}, Table 4). The viscosity of oxidised OBG37 (measured at 14 s^{-1}) was only 29% lower than that of non-oxidised OBG37 on day 7, compared to the 94% difference in viscosities of the oxidised and non-oxidised OBG85. Additionally, a clear hysteresis was observed in the stress curves of OBG37 samples (Fig. 11b).

When dissolved at 57°C, BBG had high viscosity compared to BBG dissolved at 85°C (Table 4). The viscosities of non-oxidised and oxidised BBG57 were 770 mPa·s and 50 mPa·s, respectively, on day 7 measured at 14 s^{-1}. This indicates a roughly 3-fold and 8-fold viscosity in non-oxidised and oxidised BBG57 compared to BBG85. Figure 12a also shows hysteresis of BBG57, which was more obvious in the non-oxidised sample. This behaviour differed from the behaviour of OBG37, where hysteresis was shown to be more significant in the oxidised sample (Fig. 11b).

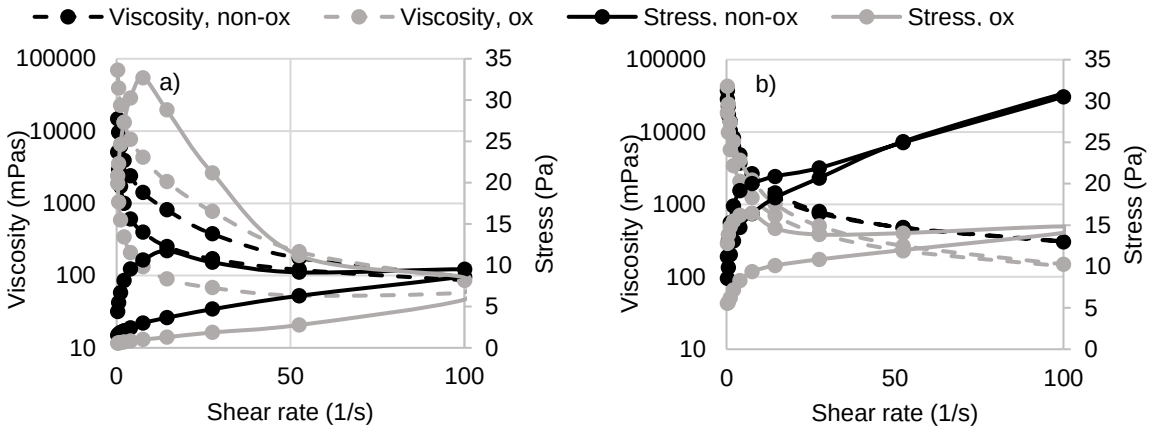

Figure 11. Viscosity and shear stress curves of non-oxidised (non-ox) and oxidised (ox) BBG37 (1.0%, w/w) (a) and OBG37 (1.5%, w/w) (b). Measurements were conducted with a rotational rheometer at 20°C using a cone-and-plate geometry on day 7. Oxidation was initiated with 70 mM H_2O_2 and 1 mM $FeSO_4 \times 7H_2O$.

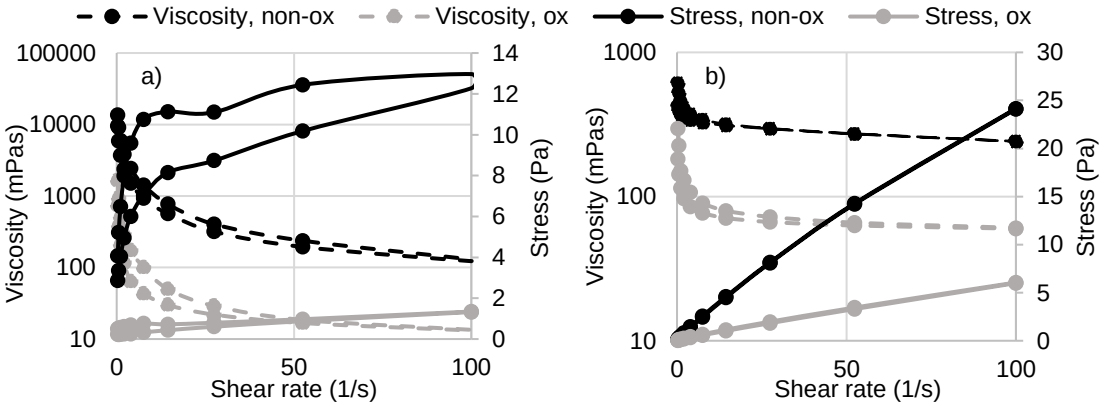

Figure 12. Viscosity and shear stress curves of non-oxidised (non-ox) and oxidised (ox) BBG57 (1.0%, w/w) (a) and OBG57 (1.5%, w/w) (b). Measurements were conducted with a rotational rheometer at 20°C using a cone-and-plate geometry on day 7. Oxidation was initiated with 70 mM H_2O_2 and 1 mM $FeSO_4 \times 7H_2O$.

No hysteresis was observed in OBG57 (Fig 12b). The viscosity of non-oxidised OBG57 did not change significantly during the storage time (Table 4). However, in oxidised OBG57 the viscosity decreased during the first day of oxidation but remained constant after that, being 100 mPa·s on day 1 and 130 mPa·s on day 7.

5.3.2.2 Oscillatory measurements

OBG37 and BBG57 were chosen for oscillatory measurements because of the hysteresis observed in the rotational measurement. Additionally, BBG37 showed hysteresis-like behaviour, but this was explained by the particles in the sample (Fig. 13a and b). Since the sample clearly was not gel-like, this sample was excluded from the oscillatory measurements, as explained in 5.3.2.1.

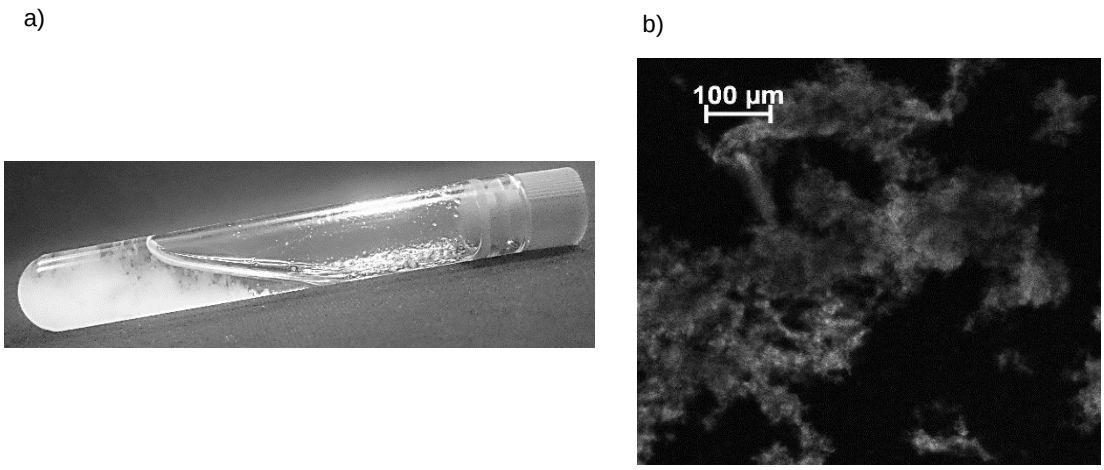

Figure 13. Photograph (a) and fluorescence microscopy image (b) showing the structure of BBG37 (1.0%, w/w) with large particles in watery medium on day 7. Adapted from study III.

Hysteresis indicating possible structure formation in OBG37 and BBG57 was confirmed by oscillatory measurements to be caused by gel formation. These tests showed gelation of both non-oxidised and oxidised OBG37 and BBG37, the storage moduli being higher than the loss moduli at all measured time points (days 1, 4 and 7) (Fig. 14 for OBG37 and Fig. 15 for BBG57). The storage moduli of non-oxidised OBG37 (Fig 14a) and BBG57 (Fig 15a) were similar, suggesting a similar gel strength of these samples. However, in oxidised samples, some difference was shown in gelation, OBG37 (Fig 14b) forming a stronger gel than BBG57 (Fig 15b). The storage modulus, *G'*, was 21 Pa in OBG37 and 3.8 Pa in BBG57 on day 7 at 1 Hz (Table 2, study III).

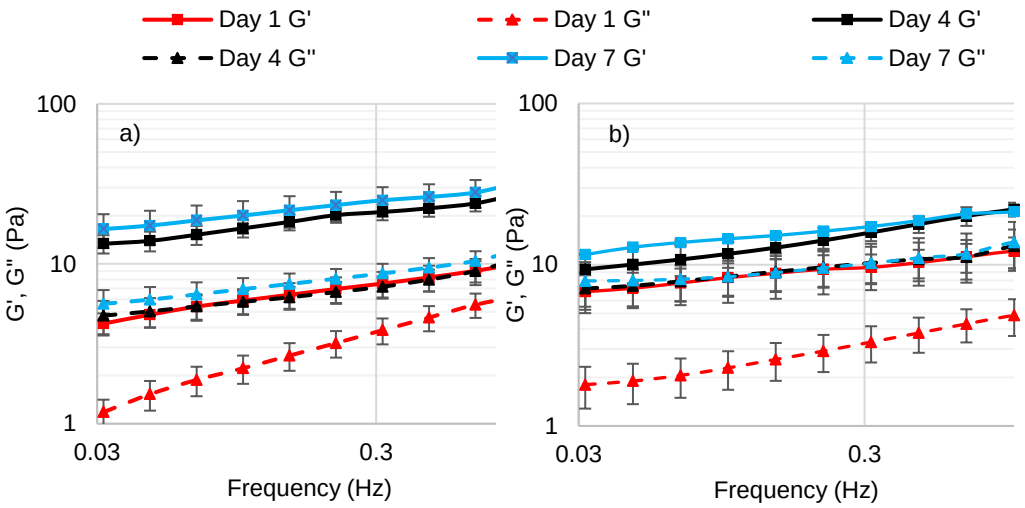

Figure 14. Storage and loss moduli (*G'* and *G"*, respectively) of non-oxidised (a) and oxidised (b) OBG37 (1.5%, w/w) on days 1, 4 and 7. Oscillatory measurement conducted at 20°C using a plate-and-plate geometry. Oxidation was initiated with 70 mM H_2O_2 and 1 mM $FeSO_4 \times 7H_2O$.

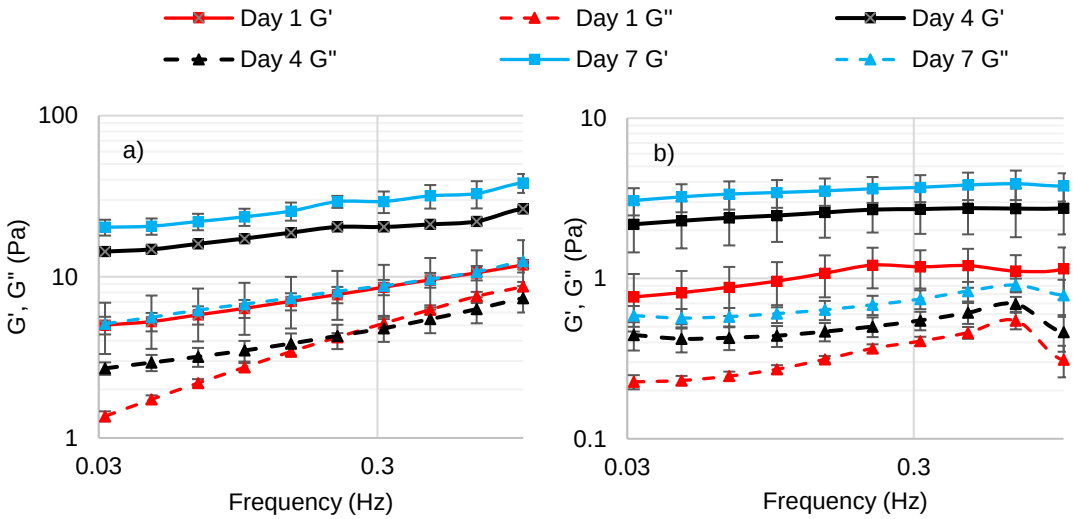

Figure 15. Storage and loss moduli (*G'* and *G"*, respectively) of non-oxidised (a) and oxidised (b) BBG57 (1.0%, w/w) on days 1, 4 and 7. Oscillatory measurement conducted at 20°C using a plate-and-plate geometry. Oxidation was initiated with 70 mM H_2O_2 and 1 mM $FeSO_4 \times 7H_2O$.

As explained in 5.3.2.1, the viscosity of oxidised OBG57 remained constant after the first oxidation day, and thus the possibility of some kind of structure formation compensating for the viscosity loss due to molar mass decrease was examined. For this reason, oscillatory measurements for non-oxidised and oxidised OBG57 were conducted, despite the lack of hysteresis in OBG57. The oscillatory measurements showed no gel formation (Figure 2, study III).

6 Discussion

Cereal β-glucan was oxidised with hydrogen peroxide, ascorbic acid and oxidised lipids. The differences in oxidation, depending on the oxidant, were investigated by studying changes in molar mass, oxidation products and structure formation (incl. aggregation and gelation). These differences are discussed here, as well as the structure formation of non-oxidised and oxidised β-glucans.

6.1 Differences in the oxidation of β-glucan with different oxidants

In all oxidation systems, Fe^{2+} ions were used as a catalyst (concentration of added $FeSO_4 \times 7H_2O$ 1 mM). Morelli et al. (2003) showed that Fe^{2+} contents of at least up to 1.5 mM did not cause significant degradation of sugars; thus added iron can be considered to act only as a catalyst in oxidation reactions.

6.1.1 Efficacy of different oxidants in oxidative degradation of β-glucan

In this study, oxidation with H_2O_2 was more efficient than with AA (Fig. 6, Table 2). In BBG this trend was obvious, but in OBG both oxidants seemed to result in rather mild degradation. However, according to Wang et al. (2017), the phytic acid content in OBG was significantly higher than in BBG (12.3 mg/g and 0.4 mg/g, respectively), which most probably resulted in less oxidation in OBG. Thus, the oxidative degradation of OBG with phytate removed was also studied. The M_w of non-oxidised pOBG was higher than the M_w of non-oxidised OBG (570 000 g/mol and 400 000 g/mol, respectively, analysed with AsFlFFF). This increase in molar mass was suggested to be caused by the phytate removal process, which included freeze-drying. Freeze-drying has been reported to decrease the solubility of barley β-glucan (Cui and Wood, 2000), in which case some aggregate formation might occur. The molar mass decrease of BBG and pOBG was similar in both AA and H_2O_2-oxidised samples, indicating that the phytic acid content in β-glucan may affect the extent of oxidation. Indeed, phytate has been shown to have an antioxidative effect mainly due to its high iron-binding capacity (Graf and Eaton, 1990).

With both H_2O_2 and AA, initiation of oxidation includes a step during which hydroxyl radicals are formed. H_2O_2 can directly decompose to form a hydroxyl radical and a hydroxide ion (Reaction 3), whereas AA requires more reaction steps when generating hydroxyl radicals (Fry, 1998; Haber and Weiss, 1934). Oxidation reactions

are pH dependent, and Fry (1998) showed oxidative scission with H_2O_2 to have a maximal rate at pH 4.5, although the reaction was still fast at pH 3.5. However, oxidation with ascorbate was significantly lower at pH 3.5 than at pH 4.5. Fry (1998) suggested that this resulted from ascorbate-mediated oxidation including an initial step during which O_2 is reduced to H_2O_2, and that this step is more efficient when ascorbate is in its mono-anion form, predominantly above pH 4.25. In the current study, the pH of both H_2O_2 and AA-oxidised samples was shown to be 3.0–3.2, which explains, at least partly, the higher oxidation rate in samples oxidised with H_2O_2 as opposed to AA.

Radical reaction products from lipid oxidation may cause co-oxidation of other macromolecules such as proteins and starch, as reviewed by Schaich et al. (2013). However, lipid radical-induced oxidation of cereal β-glucan has not previously been shown. In this study, significant oxidative degradation was observed for BBG, shown as a decrease in both the viscosity and M_w. Direct comparison between the oxidative degradation of β-glucan using hydroxyl radical-initiated oxidation and lipid-radical induced oxidation cannot be obtained from this study, since oxidation with AA and H_2O_2 was followed for 4 days and the molar mass decrease in lipid emulsion systems was measured on day 7. The maximum degradation of BBG in lipid emulsion systems was reached using HML as the oxidant, and the M_w decrease in that sample was 46% on day 7, analysed with HPSEC. Comparing this with the maximum M_w decreases during 4-day oxidation of BBG with 70 mM H_2O_2 and 70 mM AA (89% and 54%, respectively, analysed with HPSEC, Table 3), suggests that oxidation is more efficient with hydroxyl radicals from the Fenton reaction, and that the effect would probably have been even more pronounced had oxidation with H_2O_2 and AA also been continued for 7 days. When comparing hydroxyl radical-mediated oxidation to oxidation with radicals from lipid oxidation, it should be remembered that the radicals originate from different phases. Hydroxyl radicals occur in the aqueous phase and can easily reach water-soluble β-glucan molecules. Lipid oxidation occurs in the lipid phase of the system, and most likely only some of the radicals formed at this stage, will access the aqueous phase. Lipid hydroperoxides, however, may migrate to the oil-water interphase due to their surface-active nature (Berton-Carabin et al. 2014).

6.1.2 Oxidation pathways in hydroxyl radical-mediated oxidation of β-glucan

6.1.2.1 Carbonyl group formation

The significant molar mass decrease observed during hydroxyl radical-mediated oxidation of β-glucan indicated that some amount of chain scission occurred. To gain a better understanding of the pathways of β-glucan oxidation, total carbonyl contents of the CCOA-labelled samples were analysed and the equivalent amounts of reducing

end carbonyls were calculated from the M_n values. The new reducing end carbonyls were assumed to be formed during chain scission reactions and the difference between $c(C=O)_{tot}$ and $c(C=O)_{reg}$ was considered to indicate the carbonyl groups formed within the β-glucan molecules (internal carbonyl groups).

The total carbonyl group content was higher in BBG than in OBG independently of the oxidant, which correlated well with the greater molar mass decrease observed in BBG. Interestingly, there was a clear difference in carbonyl group formation in samples oxidised with H_2O_2 and AA. In both BBG and OBG, $c(C=O)_{tot}$ was significantly higher in samples oxidised with H_2O_2 than in samples oxidised with AA. Additionally, with AA, oxidation resulted mainly in formation of new reducing end carbonyl groups, while in H_2O_2-oxidised samples most of the carbonyl groups were actually internal carbonyls. Oxidation of glucose moieties in polysaccharide can result in several different radicals in the saccharide structure (Schuchmann and von Sonntag, 1977; von Sonntag, 1980). Radicals can abstract any of the six carbon-bound hydrogens in a glucosyl unit, and thus six peroxyl radicals are possible. Some of these lead to the formation of internal carbonyl or carboxyl groups and some to scission of the chain. Previous studies have reported on the radical-induced oxidation of γ-irradiated cellobiose and suggested that oxidation mainly led to radical formation at positions C1, C4 or C5, all of which would result in glycosidic cleavage (von Sonntag, 1980; von Sonntag et al., 1976). In the γ-radiolysis process, hydroxyl radicals are formed. These radicals are able to abstract the hydrogen from any carbon of the glucosyl units, and the formed radicals can undergo hydrolysis, rearrangement, elimination, or combination of these (von Sonntag et al., 1976). The radicals at C1, C4 or C5 lead mainly to hydrolysis of the glycosidic linkage. The oxidation pathways of cereal β-glucan have recently been studied, and formation of oxidised groups within the chain has also been reported (Iurlaro et al., 2014; Kivelä et al., 2012). Iurlaro et al. (2014) studied the oxidised groups in barley β-glucan with tritium-labelling, and showed that the ratio of the mid-chain oxo groups to the new reducing end groups was about 3:1. The results of our studies are consistent with their findings when it comes to BBG, since the ratio of internal carbonyls to reducing end carbonyls varied approximately from 2:1 to 3:1 in BBG samples oxidised with different concentrations of H_2O_2. In our study, OBG showed an even higher ratio of internal to reducing end carbonyls (varying approximately from 4:1 to 5:1) than BBG, but no other studies reporting this ratio for OBG were found for comparison.

6.1.2.2 Formation of formic acid and arabinose

Formic acid formation has been observed to result from the oxidation of both small saccharides and polysaccharides. Morelli et al. (2003) investigated the formic acid content of different sugars oxidised with the Fenton reaction as an indicator of oxidative damage. They showed formation of formic acid (4.4–5.2 mM) at 80°C even

without addition of H_2O_2 and ferrous ion, but the amount increased significantly with addition of about 3 mM Fe^{2+} and 15 mM H_2O_2 (6.4–10.6 mM, depending on the sugar). The highest formic acid content was observed in oxidised disaccharides and the content was 9.82 mM in oxidised maltose and 10.56 mM in oxidised sucrose. Monosaccharides had lower contents, although these were still higher than non-oxidised ones. Jin et al. (2005) proposed an oxidation pathway for polysaccharides that would lead to the formation of formic acid (Scheme 3). The first step is hydrolysis from the reducing end with cleavage of hexose (glucose in the case of β-glucan), followed by oxidation of the released hexose. The most probable position in glucose for oxidation was suggested to be the CHO group at C1, resulting in the formation of gluconic acid. This would lead to the formation of formic acid and arabonic acid via α-scission. Additionally, oxidation of the CH_2OH group can cause formic acid to develop. The lower aldonic acids formed during these reactions may further oxidise, forming more formic acid, until a total of six formic acids are cleaved from one glucose moiety.

The present study indicated formation of formic acid and arabinose in samples oxidised with H_2O_2, the concentration of these oxidation products being dependent on the concentration of H_2O_2. Free arabinose was not observed (data not shown) except after enzymatic hydrolysis. Therefore, most likely arabinose formation occurred due to oxidation of the reducing end glucose unit. In samples oxidised with AA, however, arabinose formation was not observed and formic acid contents were relatively low. The results for H_2O_2-oxidised samples partly support the theory proposed by Jin et al. (2005), as the formic acid content of oxidised β-glucan seemed to increase with an increasing amount of reducing ends in the sample. However, in oxidised β-glucans arabinose was identified instead of the arabonic acid described in Scheme 3. Thus, another degradation mechanism was considered. In the Ruff degradation, aldonic acids are decomposed in the presence of Fe^{3+} and H_2O_2 via decarboxylation to form aldose with one less carbon than the original aldonic acid (Stapley and BeMiller, 2007). In β-glucan, the reducing end glucose could oxidise to gluconic acid and form arabinose due to a decarboxylation reaction in the Ruff degradation. The reason for the absence of arabinose in AA-oxidised samples could be that AA is able to recycle Fe^{3+} formed in the Fenton reaction (Reaction 3) back to the Fe^{2+} form. As the Ruff degradation requires Fe^{3+} ions, AA could thus hinder this degradation mechanism. Our results suggest that the Ruff degradation leads to formation of arabinose during β-glucan oxidation. However, in the Ruff degradation mechanism, CO_2 is usually considered to form simultaneously with arabinose. Thus, it is not clear whether the formic acid shown in our study is from the Ruff degradation, where formic acid could be formed in some ratio instead of CO_2, or perhaps from the decomposition process explained by Jin et al. (2005). Several decomposition mechanisms may occur simultaneously and probably also CO_2 was formed in our samples though not analysed in our studies.

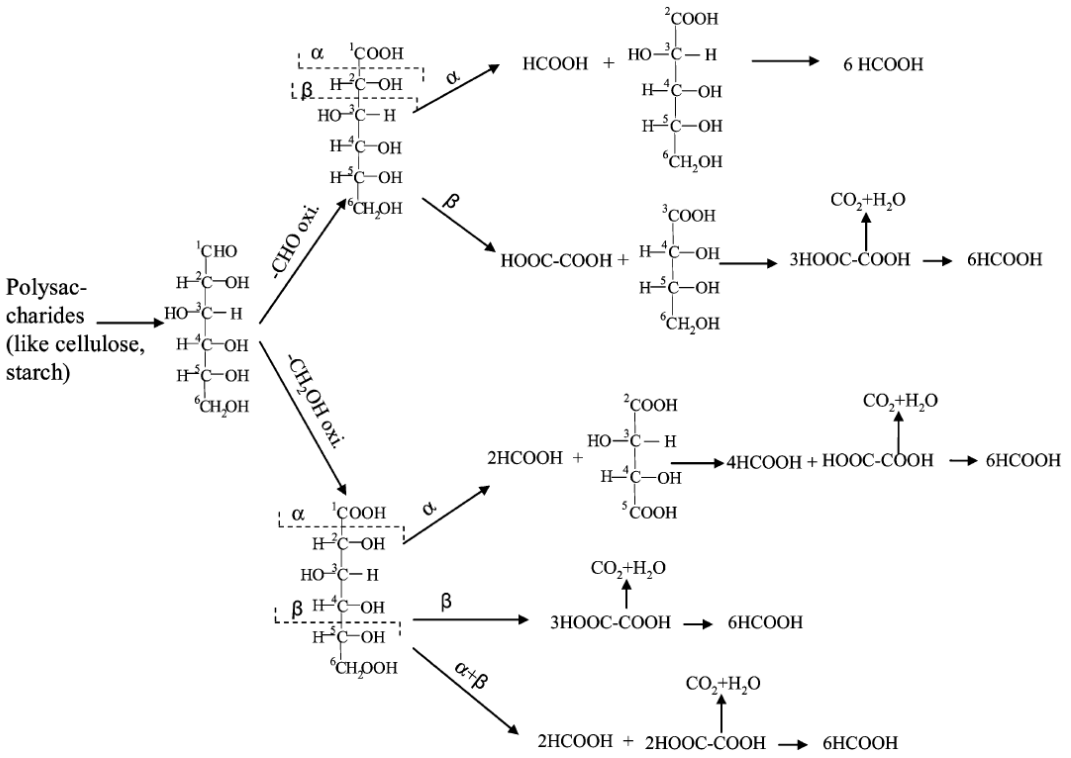

Scheme 3. Proposed mechanism for formation of formic acid and aldonic acids during oxidation reactions of polysaccharides. Adapted from Jin et al. (2005), copyrights (2005) American Chemical Society.

The results indicate that several oxidation pathways occur simultaneously. The most drastic consequence from the physiological and technological functionality perspective is probably oxidative degradation leading to scission of the chain and therefore a decrease in molar mass. Some glycosidic cleavage seems to occur also from the reducing ends, releasing glucose units that can further oxidise to produce e.g. arabinose and formic acid as observed in this study. In addition to chain scission, a significant amount of oxidised groups are formed within the chain, as only part of the carbonyl groups were shown to be reducing end carbonyls. The presence of oxidised moieties in β-glucan chains introduces more possibilities for the chains to interact with one another or with other molecules present.

6.1.3 Aggregation behaviour of oxidised β-glucan

Oxidative degradation with H_2O_2 and AA was analysed with both HPSEC and AsFlFFF. The advantage of using AsFlFFF is the ability to measure aggregated molecules and, optimally, to separate the aggregates (HM peak) from single oxidised molecules (LM peak). With HPSEC, aggregation was not observed, probably due to the solvent effect or column packing. The solvent (0.01 M LiBr/DMSO) may have caused disaggregation of the oxidised samples during HPSEC analysis. Another possible reason for disaggregation is the shearing of the molecules in the packed

column or in capillaries due to the relatively high pressure in HPSEC methods (Barth and Carlin, 1984; Maina et al., 2014; Striegel et al., 2009).

Polydispersities (M_w/M_n) were higher in AsFlFFF than in HPSEC in both non-oxidised (Table 1) and oxidised (Table 2) β-glucans, which also supports the occurrence of disaggregation in HPSEC analysis. For oxidised samples, disaggregation during analysis causes loss of information about structural changes due to oxidation. In AsFlFFF the formation of large but compact aggregates in H_2O_2-oxidised samples suggests some interaction between β-glucan molecules, possibly resulting from the internal carbonyl groups seen in CCOA-labelling. In AA-oxidised samples the aggregation was not significant, since an aggregate peak was not observed (Fig. 8), and the total M_w was significantly lower than in H_2O_2-oxidised samples. These findings correlate well with the carbonyl group data showing a comparatively low amount of internal carbonyls in AA-oxidised samples. AsFlFFF elugrams of AA-oxidised samples (example shown in Fig. 8) suggest that some amount of non-degraded molecules occur after 4 days of oxidation. However, formation of degraded molecules was also suggested by the elugram, where a shoulder appeared in the RI signal in the low molar mass area. This was in accordance with the molar mass data, which showed some decrease in total M_w.

6.2 Rheological properties of β-glucan in aqueous solutions and the effect of oxidation on these properties

Gelation of cereal β-glucan is thought to be linked to the number of cellotriosyl units in the structure (Fig. 3b), and this theory is supported by studies showing a higher gelation rate in β-glucans with higher DP3:DP4 ratio (Böhm and Kulicke, 1999b; Lazaridou et al., 2004; Tosh et al., 2004a; Wood, 2010). Based on this theory, barley β-glucan is considered to be more prone to gelation than oat β-glucan due to its higher DP3:DP4 ratio. Also, the decrease in molar mass is suggested to lead to faster gelation, since smaller molecules have higher mobility and interact with each other more quickly (Böhm and Kulicke, 1999b; Doublier and Wood, 1995). Accordingly, oxidatively degraded β-glucans should be more prone to gelation than the native ones.

However, also concentration affects gelation, as a higher concentration means a higher probability for molecules to encounter (Böhm and Kulicke, 1999b). Studies showing the relation between DP3:DP4 ratio and gelation susceptibility have had rather high concentrations, e.g. 6% (w/v) in a study by Tosh et al. (2004a) and 4–10% (w/w) in a study by Böhm and Kulicke (1999b). Lazaridou et al. (2003) reported the critical concentration for gelation of oat β-glucan with molar masses of 35 000 g/mol

and 110 000 g/mol to be 3.5% (w/w) and 4.4% (w/w), respectively. This shows the molar mass effect on gelation, and further indicates that rather high concentrations are required for low molar mass β-glucan to gel. Oat and barley β-glucans have been shown to gel at low concentration (1%) during repeated freeze-thaw cycles, a process commonly referred to as cryogelation (Lazaridou and Biliaderis, 2004). However, no studies exist showing gelation of β-glucan at these low concentrations without a cryogelation process.

In our study, the samples were dissolved at different temperatures to investigate the rheological properties of β-glucans at low concentrations with varying dissolution extents. The molar masses of BBG and OBG used in this study were different (495 000 g/mol and 361 000 g/mol, respectively, reported by the manufacturer), and the concentration of the solution (1% in BBG and 1.5% in OBG) was adjusted to compensate for this difference in respect of viscosity. As both the molar mass and concentration, as well as the DP3:DP4 ratio, influence the amount of junction zones formed in the gel and therefore also the rigidity of the gel (Böhm and Kulicke, 1999b), the differences in these factors should be considered when comparing gelation of BBG and OBG.

Based on the molar mass distribution studies of OBG and BBG, it was concluded that stirring at 85°C for 2 h was sufficient for total dissolution of soluble β-glucan. With these properly dissolved β-glucans no hysteresis or gel formation was shown, which suggests that the concentration was too low for the formation of junction zones via cellotriosyl units. Even with the molar mass decrease in oxidised samples, structure formation was not observed in BBG85 and OBG85. The viscosity of these well-solubilised β-glucans was shown to decrease with oxidation, the viscosity loss of BBG being faster than that of OBG. Faure et al. (2012) studied the hydroxyl radical formation and loss of viscosity of OBG and BBG using AA as an oxidant with ferrous iron as a catalyst. They showed faster formation of hydroxyl radicals in BBG compared to OBG during the first hours of oxidation, but after 24 h it was similar in both β-glucan samples. This early difference in the speed of radical formation could be behind the differences in the rate of viscosity loss observed in our study. Faure et al. (2012) showed a viscosity loss of 92% in BBG and 72% in OBG after 7 days of oxidation with 250 µm AA and 50 µm Fe^{2+}. In our study, this occurred already on day 1 (viscosity loss in BBG 94% and in OBG 78%) but this is reasonable when considering the higher concentration of oxidants and the use of H_2O_2 instead of AA.

Interestingly, dissolution at lower temperatures resulted in some hysteresis. The optimal dissolution temperature for structure formation was shown to differ for BBG and OBG, since hysteresis was observed in BBG57 and OBG37. These samples also had higher viscosities than the corresponding samples dissolved at 85°C, which supports the hypothesis about gel formation. Gelation of BBG57 and OBG37 was

confirmed with oscillatory measurements. The gel strengths of non-oxidised BBG57 and OBG37 did not differ significantly, and thus we concluded that the difference in the DP3:DP4 ratio did not considerably affect gelation. Alternatively, the higher concentration and lower molar mass of OBG37 compared to those of BBG57 could partially compensate for the higher gelling ability of BBG57 due to its higher DP3:DP4 ratio. The oxidised BBG57 and OBG37 samples were also shown to gel, although their gel strengths were lower than those of the corresponding non-oxidised samples. The decrease in gel strength was significantly higher in BBG57 than in OBG37, most probably due to the difference in the extent of oxidative degradation due to phytate in OBG, as discussed in 6.1.1. High viscosities were also shown for BBG37, as well as hysteresis, but this was explained by the particles in the sample rather than by gel formation. The sample contained large visible particles in a watery medium, which likely interfered with the viscosity measurements and explains the wide variation in the results.

The results of this study indicated that at low concentrations, β-glucan gelation is not entirely due to the DP3:DP4 ratio or to the higher mobility of molecules with decreased molar mass. Therefore, it was suggested that in the studied conditions, gelation was driven by the partial dissolution of β-glucan molecules. No gelation was observed in fully dissolved samples at 85°C, but it did occur with lower dissolution temperatures and it was hypothesised to result from the partially dissolved β-glucan molecules acting as nucleation sites for gelation. According to Böhm and Kulicke (1999b), junction zones are needed to form a gel network, and in the present study these were probably formed by partially dissolved parts of molecules rather than by cellotriosyl units in the β-glucan structure. Too low dissolution temperature, however, resulted in inadequate dissolution for gelation, since in BBG37 the particles were too densely packed to create a water-holding gel network.

6.3 Relevance of oxidation and structure formation for physiological and functional properties in foods

β-Glucan often occurs naturally in oat- and barley-based food products, but additionally, food products may be enriched with β-glucan-containing fractions to increase the physiological functionality of the product or to modify its technological properties. Health claims reagarding β-glucan include lowering of the postprandial glucose response and serum cholesterol levels (EFSA 2010b, 2011a, c; FDA 1997, 2005). However, physiological functionality may not be maintained in the case of depolymerisation of β-glucan or decreasing solubility, and loss of viscosity due to β-glucan degradation may compromise the stability of a food product (Wood et al., 2000).

There are several potential sources of radicals in foods that could cause oxidative degradation of β-glucan. A key factor may not be the concentration of a specific oxidant as much as the overall sum of radicals determining the extent of oxidation reactions. When considering oxidation reactions in actual food products, the presence of several oxidisable molecules must be taken into account. This study used simplified model systems to specifically investigate the oxidation reactions of cereal β-glucan and determine the effect of oxidant concentration. It therefore shows different possible oxidation products and their dependence on the oxidant and oxidant concentration. However, to be able to link these results to real products, more studies are needed to investigate e.g. differences in the susceptibility of macromolecules in foods to oxidation.

Halliwell et al. (1995) reviewed potential free radicals in foods and reported that they can originate from e.g. photosensitisation reactions or reactions with singlet oxygen. Additionally, H_2O_2 is known to be produced in the apoplast of plants (Vreeburg and Fry, 2005). Lipid peroxidation reactions can cause rancidity and off-flavours to products, but also formation of lipid radicals (Halliwell et al., 1995). H_2O_2 in food can result in the formation of hydroxyl radicals, which are the most reactive type. Additionally, hydroxyl radicals can be produced by the action of AA, as described by Fry (1998). Most of these radical reactions require a metal catalyst, which typically is present in food products as well. Thus, chemical oxidation through the formation of the radical species mentioned above is highly likely. This study showed a significant decrease in the molar masses of optimally dissolved oat and barley β-glucans due to oxidation with either H_2O_2, AA or oxidised lipids. This supports the findings of previous studies indicating that chemical oxidation may cause a molar mass decrease and consequent viscosity loss, and could thus threaten the physiological and technological functionality of cereal β-glucan (Faure et al., 2012; Kivelä et al., 2009a, b; Paquet et al., 2010).

The results of this study demonstrated the possibility of gel formation of cereal β-glucans in concentrations that are relevant for foods. Gelation at such low concentrations required an optimal dissolution temperature, and the gelation phenomenon is probably affected by the physicochemical properties, physical state and processing history of β-glucan. Interestingly, the optimal dissolution temperature was shown to be different for BBG and OBG. BBG had narrow area for the optimal temperature, with gelation observed only at 57°C. OBG had a lower optimal dissolution temperature at 37°C, and the gelation was observed in a broader temperature range. All tested temperatures in the range 35–50°C resulted in gelation of OBG, although dissolution at 37–40°C led to the strongest gel. The reason for this disparity between BBG and OBG is suggested to be differences in the energy required for partial dissolution. These findings are interesting from the functionality point of

view, because under the studied conditions the optimal dissolution temperature of OBG was found to be near the physiological temperature. This indicates that a combination of β-glucan structure and processing temperature could be optimised to enhance the physiological and technological functionality. Additionally, the results suggest that the gelation of β-glucan could overcome some of the negative effects usually linked to oxidation. Gelation may prevail over the viscosity loss resulting from decreased molar mass, as indicated especially by the viscosity of oxidised OBG37 being similar to, or higher than, that of non-oxidised OBG85 (340 mPa·s, 840 mPa·s and 1000mPa·s in oxidised OBG37 and 330 mPa·s, 330 mPa·s and 340 mPa·s in non-oxidised OBG85 on days 1, 4 and 7, respectively, measured at $14 s^{-1}$).

7 Conclusions

The physicochemical properties of β-glucan are essential for its physiological and technological functionality, which is often related to the viscosity. Degradation during processing and storage could therefore threaten the functionality of β-glucan. The present study focused on the oxidation reactions of cereal β-glucan with different oxidants. Aggregation and gelation of β-glucan and the effect of oxidation on these phenomena were also studied. The study showed significant changes in oxidation with different oxidants and the oxidation efficacy seemed to increase in the order: oxidised lipids < AA < H_2O_2. Even though oxidation was somewhat milder with radicals from lipid oxidation, this study showed for the first time that significant degradation, with consequent viscosity loss, can occur in the presence of oxidised lipids.

Oxidation pathways were further investigated with samples oxidised with AA and H_2O_2. Interestingly, these two oxidants led to different oxidation products. With AA, mostly new reducing ends were formed indicating scission of the molecules. With H_2O_2, a significant amount of internal carbonyl groups was observed in addition to chain scission, which also possibly caused aggregation of the oxidised molecules. Overall, oxidation was shown to be random and, in the case of H_2O_2, to lead to several simultaneous oxidation mechanisms including chain scission, formation of internal carbonyls and oxidation of reducing end groups.

The gelation mechanism of β-glucan at low concentrations was shown to differ from previously investigated mechanisms where at higher concentrations β-glucans with lower molar mass and higher DP3:DP4 are considered to be more susceptible to gelation. In the present study, gelation at low concentrations was shown to depend on the dissolution temperature. The results suggest that gelation required partial dissolution of the molecules, which was promoted by an optimal temperature during the dissolution process. The optimal dissolution temperature for gelation of BBG was shown to be 57°C and for that of OBG 37°C. However, gelation was observed in a wider temperature range with OBG. Oxidised BBG57 and OBG37 also gelled, although the gel strength was somewhat lower than in non-oxidised samples. The gelation results indicate that a combination of β-glucan structure and temperature during processing could possibly be optimised to provide better physiological and technological functionality in food products containing β-glucan.

This thesis provided a better understanding of the oxidation of cereal β-glucan and its role in the stability of β-glucan during processing and storage of foods containing β-glucan. The results indicate that oxidation due to radicals from various sources in food products may cause degradation of β-glucan, which is known to cause loss of

viscosity. However, the study also proposes that some of the negative effects of this viscosity loss could be overcome by the gelation of β-glucan.

There is a need for further study to clarify the factors affecting the temperature dependence of β-glucan gelation at low concentrations. The results of this study suggest that the gelation is defined by both the dissolution temperature and the structure and state of β-glucan in solution. This opens up the field to further linking the above factors to food processing and β-glucan functionality.

8 References

Ahmad A, Anjum FM, Zahoor T, Nawaz H, Ahmed Z. 2010. Extraction and characterization of β-D-glucan from oat for industrial utilization. Int J Biol Macromol 46:304–309.

Alexandratos N, Bruinsma J. 2012. World agriculture towards 2030/2050: the 2012 revision. ESA Working paper, 12-03. Rome, FAO.

Åman P, Rimsten L, Andersson R. 2004. Molecular weight distribution of β-glucan in oat-based foods. Cereal Chem 81(3):356–360.

Anderson JW, Baird P, Davis Jr RH, Ferreri S, Knudtson M, Koraym A, Waters V, Williams CL. 2009. Health benefits of dietary fiber. Nutr Rev 67(4):188–205.

Andersson AAM, Armö E, Grangeon E, Fredriksson H, Andersson R, Åman P. 2004. Molecular weight and structure units of (1 → 3, 1 → 4)-β-glucans in dough and bread made from hull-less barley milling fractions. J Cereal Sci 40:195–204.

Andersson AAM, Börjesdotter D. 2011. Effects of environment and variety on content and molecular weight of β-glucan in oats. J Cereal Sci 54:122–128.

Arts SJHF, Mombarg EJM, van Bekkum H, Sheldon RA. 1997. Hydrogen peroxide and oxygen in catalytic oxidation of carbohydrates and related compounds. Synthesis 6:597–613.

Autio K, Myllymäki O, Suortti T, Saastamoinen M, Poutanen K. 1992. Physical properties of (1→3),(1→4)-β-D-glucan preparates isolated from Finnish oat varieties. Food Hydrocolloids 5(6):513–522.

Barb WG, Baxendale JH, George P, Hargrave KR. 1951. Reactions of ferrous and ferric ions with hydrogen peroxide, part 1. – The ferrous ion reaction. Trans Faraday Soc 47:462–500.

Barbusinski K. 2009. Fenton reaction – controversy concerning the chemistry. Ecol Chem Eng S 16(3):347–358.

Barth HG. 1998. Size exclusion chromatography. In: Katz E, Eksteen R, Schoenmakers P, Miller N. Handbook of HPLC. Series: Chromatographic science 78. NY, USA: Marcel Dekker.

Barth HG, Carlin Jr FJ. 1984. A review of polymer shear degradation in size-exclusion chromatography. J Liq Chromatogr 7(9):1717–1738.

Beer MU, Wood PJ, Weisz J. 1997. Molecular weight distribution and (1 → 3)(1 → 4)-β-D-glucan content of consecutive extracts of various oat and barley cultivars. Cereal Chem 74(4):476-480.

Berton-Carabin CC, Ropers M-H, Genot C. 2014. Lipid oxidation in oil-in-water emulsions: involvement of the interfacial layer. Compr Rev Food Sci Food Saf 13:945–977.

Bhatty RS. 1995. Laboratory and pilot plant extraction and purification of β-glucans from hull-less barley and oat brans. J Cereal Sci 22:163–170.

Bingham SA, Day NE, Luben R, Ferrari P, Slimani N, Norat T, Clavel-Chapelon F, Kesse E, Nieters A, Boeing H, Tjønneland A, Overvad K, Martinez C, Dorronsoro M, Gonzalez CA, Key TJ, Trichopoulou A, Naska PV, Vineis P, Tumino R, Krogh V, Bueno-de-Mesquita HB, Peeters PHM, Berglund G, Hallmans G, Lund E, Skeie G, Kaaks R, Riboli E. 2003. Dietary fibre in food and protection against colorectal cancer in the European Prospective Investigation into Cancer and Nutrition (EPIC): an observational study. Lancet 361:1496–1501.

Böhm N, Kulicke W-M. 1999a. Rheological studies of barley (1→3)(1→4)-β-glucan in concentrated solution: investigation of the viscoelastic flow behaviour in the sol-state. Carbohydr Res 315:293–301.

Böhm N, Kulicke W-M. 1999b. Rheological studies of barley (1→3)(1→4)-β-glucan in concentrated solution: mechanistic and kinetic investigation of the gel formation. Carbohydr Res 315:302–311.

Bradley TD, Ball A, Harding SE, Mitchell JR. 1989. Thermal degradation of guar gum. Carbohydr Polym 10:205–214.

Buliga GS, Brant DA, Fincher GB. 1986. The sequence statistics and solution conformation of a barley (1→3, 1→4)-β-D-glucan. Carbohydr Res 157:139–156.

Buttriss JL, Stokes CS. 2008. Dietary fibre and health: an overview. BNF Nutr Bull 33:186–200.

Christensen BE, Ulset A-S, Beer MU, Knuckles BE, Williams DL, Fishman ML, Chau HK, Wood PJ. 2001. Macromolecular characterisation of three barley β-glucan standards by size-exclusion chromatography combined with light scattering and viscometry: an inter-laboratory study. Carbohydr Polym 45:11–22.

Cole JL, Lary JW, Moody T, Laue TM. 2008. Analytical ultracentrifugation: Sedimentation velocity and sedimentation equilibrium. Methods Cell Biol 84:143–179.

Corradini C, Cavazza A, Bignardi C. 2012. High-performance anion-exchange chromatography coupled with pulsed electrochemical detection as a powerful tool to evaluate carbohydrates of food Interest: principles and applications. Int J Carbohydr Chem 1–13.

Cui W, Wood PJ. 2000. Relationships between structural features, molecular weight and rheological properties of cereal β-D-glucan. In Nishinari K (Ed.). Hydrocolloids, Part 1. Amsterdam: Elsevier. Pp. 159–168.

Cui W, Wood PJ, Blackwell B, Nikiforuk J. 2000. Physicochemical properties and structural characterization by two-dimensional NMR spectroscopy of wheat β-D-glucan—comparison with other cereal β-D-glucans. Carbohydr Polym 41:249–258.

DeRosa MC, Crutchley RJ. 2002. Photosensitized singlet oxygen and its applications. Coord Chem Rev 233–234:351–371.

Doublier J-L, Wood PJ. 1995. Rheological properties of aqueous solutions of (1→3)(1→4)-β-D-glucan from oats (Avena sativa L.). Cereal Chem 72:335–340.

Duarte TL, Lunec J. 2005. When is an antioxidant not an antioxidant? A review of novel actions and reactions of vitamin C. In series: From Dietary Antioxidants to Regulators in Cellular Signalling and Gene Expression. Free Radical Res 39(7):671–686.

EFSA, European Food Safety Authority. 2009. Panel on dietetic products, nutrition and allergies (NDA). Scientific Opinion on the substantiation of health claims related to beta-glucans and maintenance of normal blood cholesterol concentrations (ID 754, 755, 757, 801, 1465, 2934) and maintenance or achievement of a normal body weight (ID 820, 823) pursuant to Article 13(1) of Regulation (EC) No 1924/2006. EFSA J 7(9): 1254.

EFSA, European Food Safety Authority. 2010a. Panel on dietetic products, nutrition and allergies (NDA). Scientific Opinion on dietary reference values for carbohydrates and dietary fibre. EFSA J 8(3):1462.

EFSA, European Food Safety Authority. 2010b. Panel on dietetic products, nutrition and allergies (NDA). Scientific Opinion on the substantiation of a health claim related to oat beta glucan and lowering blood cholesterol and reduced risk of (coronary) heart disease pursuant to Article 14 of Regulation (EC) No 1924/2006. EFSA J 8:1885.

EFSA, European Food Safety Authority. 2011a. Panel on dietetic products, nutrition and allergies (NDA). Scientific Opinion on the substantiation of health claims related to beta-glucans from oats and barley and maintenance of normal blood LDL-cholesterol concentrations (ID 1236, 1299), increase in satiety leading to a reduction in energy intake (ID 851, 852), reduction of post-prandial glycaemic responses (ID 821, 824), and "digestive function" (ID 850) pursuant to Article 13(1) of Regulation (EC) No 1924/2006. EFSA J 9:2207.

EFSA, European Food Safety Authority. 2011b. Panel on dietetic products, nutrition and allergies (NDA). Scientific Opinion on the substantiation of health claims related to oat and barley grain fibre and increase in faecal bulk (ID 819, 822) pursuant to Article 13(1) of Regulation (EC) No 1924/2006. EFSA Jl 9:2249.

EFSA, European Food Safety Authority. 2011c. Panel on dietetic products, nutrition and allergies (NDA). Scientific Opinion on the substantiation of a health claim related to barley beta-glucans and lowering of blood cholesterol and reduced risk of (coronary) heart disease pursuant to Article 14 of Regulation (EC) No 1924/2006. EFSA J 9:2471.

Faure AM, Andersen ML, Nyström L. 2012. Ascorbic acid induced degradation of beta-glucan: hydroxyl radicals as intermediates studied by spin trapping and electron spin resonance spectroscopy. Carbohydr Polym 87:2160–2168.

Faure AM, Werder J, Nyström L. 2013. Reactive oxygen species responsible for beta-glucan degradation. Food Chem 141:589–596.

FDA, Food and Drug Administration, Department of Health and Human Services (HHS). 1997. Food labeling: Health claims; Oats and coronary heart disease. Final Rule. Fed Regist 62(15):3584–3601.

FDA, Food and Drug Administration, Department of Health and Human Services (HHS). 2005. Food labeling: Health claims; Soluble dietary fiber from certain foods and coronary heart disease. Final Rule. Fed Regist 70(246):76150–76162.

Fenton HJH. 1894. LXXIII. Oxidation of tartaric acid in presence of iron. J Chem Soc, Trans 65:899-910.

Fincher GB. 1989. Molecular and cellular biology associated with endosperm mobilization in germinating cereal grains. Annu Rev Plant Physiol Plant Mol Biol 40:305–46.

Fincher GB. 1993. Structure-function relatioships of β-glucan hydrolases in barley. In: Meuser F, Manners DJ, Seibel W. Plant Polymeric Carbohydrates. Special Publication 134. UK: The Royal Society of Chemistry.

Fincher GB, Stone BA. 1986. Cell walls and their components in cereal grain technology. Adv Cereal Sci and Technol, 8:207–295.

Fry SC. 1998. Oxidative scission of plant cell wall polysaccharides by ascorbate-induced hydroxyl radicals. Biochem J 332:507–515.

Giddings JC. 1994. Universal calibration in size exclusion chromatography and thermal field-flow fractionation. Anal Chem 66:2783-2787.

Giddings JC. 2000. The field-flow fractionation family: Underlying principles. In Schimpf M, Caldwell K, Giddings JC (Eds.), Field-Flow Fractionation Handbook. New York: John Wiley & Sons. Pp. 3–30.

Gilbert BC, King DM, Thomas B. 1984. The oxidation of some polysaccharides by the hydroxyl radical: an E.S.R. investigation. Carbohydr Res 125:217–235.

Gómez C, Navarro A, Manzanares P, Horta A, Carbonell JV. 1997. Physical and structural properties of barley (1→3),(1→4)-β-D-glucan. Part I. Determination of molecular weight and macromolecular radius by light scattering. Carbohydr Polym 32:7–15.

Gooding KM, Regnier FE. 2002. Size exclusion chromatography. In: Gooding KM, Regnier FE. HPLC of Biological Macromolecules. 2nd Edition. NY, USA: Marcel Dekker. Pp 49–80.

Graf E, Eaton JW. 1990. Antioxidant functions of phytic acid. Free Radical Biol Med 8:61–69.

Grimm A, Krüger E, Burchard W. 1995. Solution properties of β-D-(1,3)(1,4)-glucan isolated from beer. Carbohydr Polym 27:205–214.

Guo B, Yuan Y, Wu Y, Xie Q, Yao S. 2002. Assay and analysis for anti- and pro-oxidative effects of ascorbic acid on DNA with the bulk acoustic wave impedance technique. Anal Biochem 305:139–148.

Haber F, Weiss J. 1934. The catalytic decomposition of hydrogen peroxide by iron salts. Proc R Soc A 147:332–351.

Halliwell B, Gutteridge JMC. 1984. Oxygen toxicity, oxygen radicals, transition metals and disease. Biochem J 219:1–14.

Halliwell B, Murcia MA, Chirico S, Aruoma OI. 1995. Free radicals and antioxidants in food and in vivo: What they do and how they work. Crit Rev Food Sci Nutr 35(1-2):7–20.

Harding SE, Jumel K. 2001. Light scattering. Curr Protoc Protein Sci 11:7.8: 7.8.1–7.8.14.

Harding SE, Vårum KM, Stokke BT, Smidsrød O. 1991. Molecular weight determination of polysaccharides. Adv Carbohydr Anal 1: 63–144.

Hrmova M, Fincher GB. 2001. Structure-function relationships of β-D-glucan endo- and exohydrolases from higher plants. Plant Mol Biol 47:73–91.

Iurlaro A, Dalessandro G, Piro G, Miller JG, Fry SC, Lenucci MS. 2014. Evaluation of glycosidic bond cleavage and formation of oxo groups in oxidized barley mixed-linkage β-glucans using tritium labelling. Food Res Int 66:115–122.

Izydorczyk MS, Macri LJ, MacGregor AW. 1998. Structure and physicochemical properties of barley non-starch polysaccharides - I. Water-extractable β-glucans and arabinoxylans. Carbohydr Polym 35:249–258.

Jin F, Zhou Z, Moriya T, Kishida H, Higashijima H, Enomoto H. 2005. Controlling hydrothermal reaction pathways to improve acetic acid production from carbohydrate biomass. Environ Sci Technol 39:1893–1902.

Johansson L, Virkki L, Anttila H, Esselström H, Tuomainen P, Sontag-Strohm T. 2006. Hydrolysis of β-glucan. Food Chem 97:71–79.

Johansson L, Virkki L, Maunu S, Lehto M, Ekholm P, Varo P. 2000. Structural characterization of water soluble β-glucan of oat bran. Carbohydr Polym 42:143–148.

Kaczmarczyk MM, Miller MJ, Freund GG. 2012. The health benefits of dietary fiber: Beyond the usual suspects of type 2 diabetes mellitus, cardiovascular disease and colon cancer. Metab Clin Exp 61: 1058–1066.

Kanner J. 2010. Metals and food oxidation. In Decker EA, Elias RJ, McClements, DJ. Oxidation in Foods and Beverages and Antioxidant Applications, Volume 1 - Understanding Mechanisms of Oxidation and Antioxidant Activity. UK: Woodhead Publishing. Pp 36–56.

Kearney J. 2010. Food consumption trends and drivers. Philos Trans R Soc, B 365:2793–2807.

Kivelä R. 2011. Non-enzymatic degradation of (1→3)(1→4)-β-D-glucan in aqueous processing of oats. Doctoral thesis, University of Helsinki. Unigrafia.

Kivelä R, Gates F, Sontag-Strohm T. 2009a. Rapid Communication. Degradation of cereal beta-glucan by ascorbic acid induced oxygen radicals. J Cereal Sci 49:1–3.

Kivelä R, Henniges U, Sontag-Strohm T, Potthast A. 2012. Oxidation of oat β-glucan in aqueous solutions during processing. Carbohydr Polym 87:589–597.

Kivelä R, Nyström L, Salovaara H, Sontag-Strohm T. 2009b. Role of oxidative cleavage and acid hydrolysis of oat beta-glucan in modelled beverage conditions. J Cereal Sci 50:190–197.

Knill CJ, Kennedy JF. 2003. Degradation of cellulose under alkaline conditions. Carbohydr Polym 51:281–300.

Kremer ML. 2003. The Fenton reaction. Dependence of the rate on pH. J Phys Chem A 107:1734–1741.

Lampi A-M, Dimberg LH, Kamal-Eldin A. 1999. A study on the influence of fucosterol on thermal polymerisation of purified high oleic sunflower triacylglycerols. J Sci Food Agric 79(4):573–579.

Lazaridou A, Biliaderis CG. 2004. Cryogelation of cereal β-glucans: structure and molecular size effects. Food Hydrocolloids 18:933-947.

Lazaridou A, Biliaderis CG. 2007. Molecular aspects of cereal β-glucan functionality: physical properties, technological applications and physiological effects. J Cereal Sci 46:101–118.

Lazaridou A, Biliaderis CG, Izydorczyk MS. 2003. Molecular size effects on rheological properties of oat β-glucans in solution and gels. Food Hydrocolloids 17:693–712.

Lazaridou A, Biliaderis CG, Micha-Screttas M, Steele BR. 2004. A comparative study on structure–function relations of mixed-linkage (1 → 3), (1 → 4) linear β-D-glucans. Food Hydrocolloids 18:837–855.

Lazaridou A, Marinopoulou A, Matsoukas NP, Biliaderis CG. 2014. Impact of flour particle size and autoclaving on β-glucan physicochemical properties and starch digestibility of barley rusks as assessed by *in vitro* assays. Bioact Carbohydr Diet Fibre 4:58–73.

Lee YC. 1990. High-performance anion-exchange chromatography for carbohydrate analysis. Anal Biochem 189:151–162.

Li W, Cui SW, Wang Q, Yada RY. 2011. Studies of aggregation behaviours of cereal β-glucans in dilute aqueous solutions by light scattering: Part I. Structure effects. Food Hydrocolloids 25(2):189–195.

Løgager T, Holcman J, Sehested K, Pedersen T. 1992. Oxidation of ferrous ions by ozone in acidic solutions. Inorg Chem 31(17):3523–3529.

Luchsinger WW, Stone BA. 1976. Linkage sequencing of oligosaccharides by their rates of alkaline degradation. Carbohydr Res 46(1):1–8.

Maina NH, Pitkänen L, Heikkinen S, Tuomainen P, Virkki L, Tenkanen M. 2014. Challenges in analysis of high-molar mass dextrans: Comparison of HPSEC, AsFlFFF and DOSY NMR spectroscopy. Carbohydr Polym 99:199–207.

Mälkki Y, Virtanen E. 2001. Gastrointestinal effects of oat bran and oat gum, a review. Lebensm Wiss Technol 34:337–347.

Mewis J, Wagner NJ. 2009. Thixotropy. Adv Colloid Interface Sci 147–148:214–227.

Mitchell JR. 1980. The rheology of gels. J Texture Stud 11:315–337.

Morelli R, Russo-Volpe S, Bruno N, Lo Scalzo R. 2003. Fenton-dependent damage to carbohydrates: free radical scavenging activity of some simple sugars. J Agric Food Chem 51(25):7418–7425.

Morris ER, Cutler AN, Ross-Murphy SB, Rees DA, Price J. 1981. Concentration and shear rate dependence of viscosity in random coil polysaccharide solutions. Carbohydr Polym 1(1):5–21.

Myers MN, Oppenheimer LE, Schimpf ME. 2000. Ancillary equipment. In Schimpf M, Caldwell K, Giddings JC (Eds.), Field-Flow Fractionation Handbook. New York: John Wiley & Sons. Pp. 213–224.

Othman RA, Moghadasian MH, Jones PJH. 2011. Cholesterol-lowering effects of oat β-glucan. Nutr Rev 69(6):299–309.

Paquet E, Turgeon SL, Lemieux S. 2010. Effect of xanthan gum on the degradation of cereal β-glucan by ascorbic acid. J Cereal Sci 52(2):260–262.

Pavasars I, Hagberg J, Borén H, Allard B. 2003. Alkaline degradation of cellulose: Mechanisms and kinetics. J Polym Environ 11(2):39–47.

Picout DR, Ross-Murphy SB. 2003. Rheology of biopolymer solutions and gels. Sci World J 3:105–121.

Pielichowski K, Njuguna J. 2005. Thermal degradation of polymeric materials. UK: Rapra Technology Ltd.

Potthast A, Radosta S, Saake B, Lebioda S, Heinze T, Henniges U, Isogai A, Koschella A, Kosma P, Rosenau T, Schiehser S, Sixta H, Strlič M, Strobin G, Vorwerg W, Wetzel H. 2015. Comparison testing of methods for gel permeation chromatography of cellulose: coming closer to a standard protocol. Cellulose 22:1591–1613.

Qian SY, Buettner GR. 1999. Iron and dioxygen chemistry is an important route to initiation of biological free radical oxidations: an electron paramagnetic resonance spin trapping study. Free Radical Biol Med 26(11):1447–1456.

Qin F, Kes M, Christensen BE. 2013. A study of bioactive, branched (1 → 3)-β-D-glucans in dimethylacetamide/LiCl and dimethyl sulphoxide/LiCl using size-exclusion chromatography with multi-angle light scattering detection. J Chromatogr A 1305:109–113.

Ragaee SM, Wood PJ, Wang Q, Tosh S, Brummer Y. 2008. Extractability, structure and molecular weight of β-glucan from Canadian rye (*Secale cereale* L.) whole meal. Cereal Chem 85(3):283–288.

Ratanathanawongs-Williams SK. 2000. Flow field-flow fractionation. In Schimpf M, Caldwell K, Giddings JC (Eds.), Field-Flow Fractionation Handbook. New York: John Wiley & Sons. Pp. 257–278.

Röhrling J, Potthast A, Rosenau T, Lange T, Borgards A, Sixta H, Kosma P. 2002b. A novel method for the determination of carbonyl groups in cellulosics by fluorescence labeling. 2. Validation and applications. Biomacromolecules 3:969–975.

Röhrling J, Potthast A, Rosenau T, Lange T, Ebner G, Sixta H, Kosma P. 2002a. A novel method for the determination of carbonyl groups in cellulosics by fluorescence labeling. 1. Method development. Biomacromolecules 3:959–968.

Schaich KM, Shahidi F, Zhong Y, Eskin NAM. 2013. Lipid oxidation. In Eskin NAM, Shahidi F (Eds.). Biochemistry of Foods. 3rd Edition. USA: Academic Press, Elsevier. Pp 419–478.

Schuchmann MN, von Sonntag C. 1977. Radiation chemistry of carbohydrates. Part 14. Hydroxyl radical induced oxidation of D-glucose in oxygenated aqueous solution. J Chem Soc, Perkin Trans 2:1958–1963.

Scott KP, Duncan SH, Flint HJ. 2008. Dietary fibre and the gut microbiota. BNF Nutr Bull 33(3):201–211.

Skendi A, Biliaderis CG, Lazaridou A, Izydorczyk MS. 2003. Structure and rheological properties of water soluble β-glucans from oat cultivars of *Avena sativa* and *Avena bysantina*. J Cereal Sci 38:15–31.

Skibsted LH. 2010. Understanding oxidation processes in foods. In Decker EA, Elias RJ, McClements, DJ. Oxidation in Foods and Beverages and Antioxidant Applications, Volume 1 - Understanding Mechanisms of Oxidation and Antioxidant Activity. UK: Woodhead Publishing. Pp 3–35.

von Sonntag C. 1980. Free-radical reactions of carbohydrates as studied by radiation techniques. Adv Carbohydr Chem Biochem 37:7–77.

von Sonntag C, Dizdaroglu M, Schulte-Frohlinde D. 1976. Radiation chemistry of carbohydrates, Vlll. γ-Radiolysis of cellobiose in N_2O-saturated aqueous solution. Part II. Quantitative measurements, mechanisms of the radical-induced scission of the glycosidic linkage. Z Naturforsch B, 31(6):857-864.

Stapley JA, BeMiller JN. 2007. The Ruff degradation: a review of previously proposed mechanisms with evidence that the reaction proceeds by a Hofer–Moest-type reaction. Carbohydr Res 342:407–418.

Simmons TJ, Uhrín D, Gregson T, Murray L, Sadler IH, Fry SC. 2013. An unexpectedly lichenase-stable hexasaccharide from cereal, horsetail and lichen mixed-linkage β-glucans (MLGs): Implications for MLG subunit distribution. Phytochemistry 95:322–332.

Striegel AM, Yau WW, Kirkland JJ, Bly DD. 2009. Modern Size-Exclusion Liquid Chromatography. 2nd Edition. NJ, USA: John Wiley & Sons.

Sundberg B, Wood P, Lia Å, Andersson H, Sandberg A-S, Hallmans G, Åman P. 1996. Mixed-linked β-glucan from breads of different cereals is partly degraded in the human ileostomy model. Am J Clin Nutr 64:878–885.

Tosh SM, Brummer Y, Wood PJ, Wang Q, Weisz J. 2004a. Evaluation of structure in the formation of gels by structurally diverse (1→3)(1→4)-β-D-glucans from four cereal and one lichen species. Carbohydr Polym 57:249–259.

Tosh SM, Wood PJ, Wang Q, Weisz J. 2004b. Structural characteristics and rheological properties of partially hydrolyzed oat β-glucan: the effects of molecular weight and hydrolysis method. Carbohydr Polym 55:425–436.

Tvaroska I, Ogawa K, Deslandes Y, Marchessault RH. 1983. Crystalline conformation and structure of lichenan and barley β-glucan. Can J Chem 61(7):1608-1616.

Ueda S, Hayashi T, Namiki M. 1986. Effect of ascorbic acid on lipid autoxidation in a model food system. Agric Biol Chem 50(1):1–7.

Vaikousi H, Biliaderis CG. 2005. Processing and formulation effects on rheological behavior of barley β-glucan aqueous dispersions. Food Chem 91:505–516.

Vårum KM, Smidsrød O, Brant DA. 1992. Light scattering reveals micelle-like aggregation in the (1→ 3),(1→ 4)-β-D-glucans from oat aleurone. Food Hydrocolloids 5(6):497–511.

Vasanthan T, Temelli F. 2008. Grain fractionation technologies for cereal beta-glucan concentration. Food Res Int 41:876–881.

Villetti MA, Crespo JS, Soldi MS, Pires ATN, Borsali R, Soldi V. 2002. Thermal degradation of natural polymers. J Therm Anal Calorim 67(2):295–303.

Vreeburg RAM, Fry SC. 2005. Reactive oxygen species in cell walls. In Smirnoff N (Ed.), Antioxidants and reactive oxygen species in plants. Oxford: Blackwell Publishing Ltd. Pp. 215–249.

Wahlund K-G. 2000. Asymmetrical flow field-flow fractionation. In Schimpf M, Caldwell K, Giddings JC (Eds.), Field-Flow Fractionation Handbook. New York: John Wiley & Sons. Pp. 279–294.

Walling C. 1998. Intermediates in the reactions of Fenton type reagents. Acc Chem Res 31(4):155–157.

Wang Q, Ellis PR, Ross-Murphy SB. 2000. The stability of guar gum in an aqueous system under acidic conditions. Food Hydrocolloids 14(2):129–134.

Wang Q, Wood PJ, Cui W, Ross-Murphy SB. 2001. The effect of autoclaving on the dispersibility and stability of three neutral polysaccharides in dilute aqueous solutions. Carbohydr Polym 45: 355–362.

Wang Y-J, Maina NH, Ekholm P, Lampi A-M, Sontag-Strohm T. 2017. Retardation of oxidation by residual phytate in purified cereal β-glucans. Food Hydrocolloids 66:161–167.

Wen J, Arakawa T, Philo JS. 1996. Size-exclusion chromatography with on-line light-scattering, absorbance, and refractive index detectors for studying proteins and their interactions. Anal Biochem 240(2):155–166.

Wood PJ. 2010. Review. Oat and rye β-glucan: properties and function. Cereal Chem 87:315–330.

Wood PJ, Beer MU, Butler G. 2000. Evaluation of role of concentration and molecular weight of oat β-glucan in determining effect of viscosity on plasma glucose and insulin following an oral glucose load. Br J Nutr 84(1):19–23.

Wood PJ, Braaten JT, Scott FW, Riedel KD, Wolynetz MS, Collins MW. 1994. Effect of dose and modification of viscous properties of oat gum on plasma glucose and insulin following an oral glucose load. Br J Nutr 72(5):731–743.

Wu J, Zhang Y, Wang L, Xie B, Wang H, Deng S. 2006. Visualization of single and aggregated hulless oat (*Avena nuda* L.)(1→ 3),(1→ 4)-β-D-glucan molecules by atomic force microscopy and confocal scanning laser microscopy. J Agric Food Chem 54(3):925–934.

Yohannes G. 2007. Asymmetrical flow field-flow fractionation in the study of water-soluble macromolecules. Doctoral thesis, University of Helsinki. Helsinki University Printing House.

Zohuriaan MJ, Shokrolahi F. 2004. Thermal studies on natural and modified gums. Polym Test 23(5):575–579.